The Magnitude and IgG Subclass of Antibodies Elicited by Targeted DNA Vaccines Are Influenced by Specificity for APC Surface Molecules

Ranveig Braathen, Heidi C. L. Spång, Mona M. Lindeberg, Even Fossum, Gunnveig Grødeland, Agnete B. Fredriksen and Bjarne Bogen

ImmunoHorizons 2018, 2 (1) 38-53
doi: https://doi.org/10.4049/immunohorizons.1700038
http://www.immunohorizons.org/content/2/1/38

ImmunoHorizons is an open access journal published by
The American Association of Immunologists, Inc.,
1451 Rockville Pike, Suite 650, Rockville, MD 20852

ISSN 2573-7732.

ImmunoHorizons

RESEARCH ARTICLE

Adaptive Immunity

The Magnitude and IgG Subclass of Antibodies Elicited by Targeted DNA Vaccines Are Influenced by Specificity for APC Surface Molecules

Ranveig Braathen,* Heidi C. L. Spång,* Mona M. Lindeberg,* Even Fossum,* Gunnveig Grødeland,* Agnete B. Fredriksen,*,[1] and Bjarne Bogen*,[†]

*K.G. Jebsen Centre for Influenza Vaccine Research, Institute of Clinical Medicine, University of Oslo and Oslo University Hospital, 0027 Oslo, Norway; and [†]Centre for Immune Regulation, Institute of Immunology, University of Oslo and Oslo University Hospital, 0027 Oslo, Norway

ABSTRACT

Upon APC-targeted DNA vaccination, transfected cells secrete fusion proteins with targeting units specific for surface molecules on APC. In this study, we have tested several different targeting units for their ability to influence the magnitude and subclass of Ab responses to hemagglutinin from influenza A virus. The experiments employed bivalent homodimeric Ig-based molecules (vaccibodies). The overall efficiency in BALB/c mice depended on the targeting units in the following order: αMHC class II > αCD11c > αCD40 > Xcl-1 = MIP-1α > FliC > GM-CSF > Flt-3L > αDEC205. GM-CSF induced mainly IgG1, whereas Xcl1, MIP-1α, αCD40, and αDEC205 induced predominantly IgG2a. A more balanced mixture of IgG1 and IgG2a was observed with αCD11c, αMHC class II, Flt-3L, and FliC. Similar results of IgG subclass–skewing were obtained in Th1-prone C57BL/6 mice with a more limited panel of vaccines. IgG1 responses in BALB/c occurred early after immunization but declined relatively rapidly over time. IgG2a responses appeared later but lasted longer (>252 d) than IgG1 responses. The most efficient targeting units elicited short- and long-term protection against PR8 influenza (H1N1) virus in BALB/c mice. The results suggest that targeting of $Xcr1^+$ conventional type 1 dendritic cells preferentially induces IgG2a responses, whereas simultaneous targeting of several dendritic cell subtypes also induces IgG1 responses. The induction of distinct subclass profiles by different surface molecules supports the APC–B cell synapse hypothesis. The results may contribute to generation of more potent DNA vaccines that elicit high levels of Abs with desired biologic effector functions. *ImmunoHorizons*, 2018, 2: 38–53.

INTRODUCTION

Most successful vaccines owe their efficacy to the induction of protective Abs (1). Thus, a major aim must be to generate vaccine formats that induce high and long-lasting Ab responses with appropriate biological effector functions.

Conventional vaccines typically contain attenuated or inactivated pathogens. Nevertheless, subunit vaccines are attractive due to their safety profile and ability to focus immune responses toward the Ag of interest. Subunit vaccines have a number of advantages, but suffer from low immunogenicity, hence, their efficiency needs to be improved. Subunit vaccines

Received for publication August 9, 2017. Accepted for publication December 21, 2017.

Address correspondence and reprint requests to: Dr. Ranveig Braathen and Prof. Bjarne Bogen, K.G. Jebsen Centre for Influenza Vaccine Research, Institute of Clinical Medicine, University of Oslo and Oslo University Hospital, 0027 Oslo, Norway. E-mail addresses: ranveig.braathen@medisin.uio.no (R.B.) and bjarne.bogen@medisin.uio.no (B.B.)

ORCID: 0000-0003-0451-5936 (R.B.).

[1]Current address: Vaccibody AS, Oslo Research Park, Oslo, Norway.

This work was supported by the Research Council of Norway, Helse Sør-Øst (Regional Health Authority), and the K.G. Jebsen Foundation.

Abbreviations used in this article: cDC1, conventional dendritic cell type 1; DC, dendritic cell; HA, hemagglutinin; HEK, human embryonic kidney; m, murine; Mφ, macrophage; MHCII, MHC class II; NIP, 5-iodo-4-hydroxy-3-nitrophenylacetyl; scFv, single-chain fragment variable.

The online version of this article contains supplemental material.

https://doi.org/10.4049/immunohorizons.1700038

ImmunoHorizons is published by The American Association of Immunologists, Inc.

may be delivered either as proteins in adjuvants or as DNA. DNA vaccines are attractive due to their ease of construction and cost-effective manufacture (2). However, although DNA vaccines are efficient in rodents and some larger animals such as dogs (3) and horses (4), immune responses in humans have so far been disappointing (5).

Traditionally, DNA vaccines have been used to induce T cell responses (2). However, DNA vaccination in certain formats can induce high amount of Abs as well. One such Ab-enhancing format combines DNA vaccination with targeting of Ag to APC. This is achieved by the construction of DNA plasmids encoding secreted fusion proteins that target APC for increased delivery of Ag, resulting in improved immune responses (6–9). In this study this principle is called a targeted DNA vaccine.

For targeted DNA vaccines to induce Abs, it is important that the included Ags express conformation-dependent antigenic determinants recognized by the BCR of B cells (10). Moreover, induction of Abs appears to be enhanced if plasmids encode dimeric (rather than monomeric) APC-targeting fusion proteins, presumably due to a need for cross-linking of BCRs (11). To fulfill these prerequisites, in our previous studies DNA vaccines have encoded homodimeric vaccine proteins (vaccibodies), where each chain contains a targeting unit and an antigenic unit, thus affording bivalency both with regard to binding to APC surface molecules and BCR recognition.

Because APC targeting increases Ab levels elicited by DNA vaccines, it has been suggested that vaccine proteins bridge an APC and a responding B cell (12, 13). Circumstantial evidence supports the formation of APC–B cell synapsis during immune responses (14–17). In such a putative APC–B cell synapse, the targeting units of the vaccine protein bind surface molecules on the APC whereas the antigenic parts bind BCRs of the responding B cell (10, 12). If the bivalent APC-targeted vaccine proteins really function via an APC–B cell synapsis, one would expect that the magnitude and subclass profiles of Ab responses could be influenced by the type and density of targeted surface molecules, as well as receptor expression profile on different APC subtypes. This study was undertaken to address these issues.

Targeted DNA vaccibody vaccines have previously been constructed with different APC-specific units such as single-chain fragment variable (scFv) specific for MHC class II (MHCII) (8, 13) or CD40 (9), or chemokines such as MIP-1α (11, 18) or Xcl1 (19). These targeted DNA vaccines have resulted in different levels of Abs (besides inducing T cells). However, the relative efficiencies of the various targeting units have not been directly compared. In this study we have performed a side-by-side comparison of these previous targeted DNA vaccines in an influenza model using hemagglutinin (HA) as Ag. In addition, we have included a number of new targeting units in the vaccibody format (GM-CSF, Flt-3L, FliC, αCD11c, αDEC205). The study shows that magnitude, subclass, and duration of induced IgG Abs, as well as protection against influenza, are heavily influenced by the targeting units employed. The results may be useful for generating more potent DNA vaccines that induce high levels of IgG Abs with desired biologic effector mechanisms.

MATERIALS AND METHODS

Mice, cell lines, and influenza viruses

BALB/c and C57BL/6 mice were obtained from Taconic, Denmark. The experimental protocol was approved by the Norwegian Animal Research Authority (Oslo, Norway). Human embryonic kidney (HEK) 293E cells and the macrophage (Mφ) J774A.1 cell line were purchased from American Type Culture Collection (Manassas, VA). Cells were cultured in RPMI 1640 (Invitrogen) and DMEM (Invitrogen) respectively, supplemented with 10% heat-inactivated FCS (Biochrom AG), 0.1 mM nonessential amino acids (Lonza), 1 mM natrium pyruvate (Lonza), 50 μM monothioglycerol (Sigma-Aldrich), and 40 mg/ml Gensumycin (Sanofi-Avensis Norway), at 37°C with 5% CO_2 in humidified air. Influenza virus strain A/PR/8/34 (H1N1) was kindly provided by Dr. A.G. Hauge at the National Veterinary Institute, Oslo, Norway.

Cloning of the various targeting plasmid vectors

The basic vaccine construct containing a human dimerization unit consisting of hinge 1 and hinge 4 as well as $C_\gamma3$ from human IgG3 has been previously described (8) (see Fig. 1A, 1B). The vaccine constructs containing the HA Ag from influenza A virus [A/Puerto Rico/8/34 (H1N1)] as the antigenic unit, and the targeting units mouse MIP-1α (NM_011337.2), anti–I-E^d ($scFv^{anti\text{-}I\text{-}Ed}$, from mouse 14-4-4S anti-MHCII mAb specific for the Ia.7 determinant on E_α chains), or anti–5-iodo-4-hydroxy-3-nitrophenylacetyl (NIP) ($scFv^{anti\text{-}NIP}$ from mouse B1-8 mAb specific for the hapten NIP), have previously been published (13, 18). All these constructs contained the V_H-leader derived from V_H-gene of B1-8 originally included in the pLNOH2 vector (20). The targeting units anti-CD40 ($scFv^{anti\text{-}CD40}$, clone FGK-45) (9) and mouse Xcl1 (NP_032536.1) (19) were subcloned into the unique restriction sites *Bsm*I and *Bsi*WI of the pLNOH2 vector. The mouse GM-CSF (GenBank: X02333.1), Flt-3L (mouse Fms-like tyrosine kinase receptor-3 ligand, GenBank: L23636.1), and *fliC* (*fliC*/flagellin from *Salmonella typhimurium*, GenBank: D13689.1) genes were amplified with PCR. The specific primers used were: 5′mGM-CSF: 5′-GGT GTG CAT TCC GCA CCC ACC CGC TCA CCC-3′, 3′mGM-CSF: 5′-GAC GTA CGA CTC ACC TTT TTG GCT TGG TTT TTT GCA CTC-3′, 5′Flt-3L: 5′-GGT GTG CAT TCC GGG ACA CCT GAC TGT TAC TTC-3′, 3′Flt-3L: 5′-GAC GTA CGA CTC ACC TCT GGG CCG AGG CTC TGGG-3′, 5′*fliC*: 5′-GGT GTG CAT TCC ATG GCA CAA GTC ATT AAT ACA AAC-3′ and 3′*fliC*: 5′-GAC GTA CGA CTC ACC TCG CAG TAA AGA GAG GAC GTT-3′. The PCR products were subcloned into the unique restriction sites *Bsm*I and *Bsi*WI in the pLNOH2 vector containing the dimerization domain and HA. The murine (m) GM-CSF gene contained one internal BsmI site that was removed with quick-change mutagenesis PCR (the primers used were: 5′mGM-CSF QC BsmI: 5′-CTG ATA TCC CCT TTG AGT GCA AAA AAC CAA GCC-3′ and 3′mGM-CSF QC BsmI: 5′-GGC TTG GTT TTT TGC ACT CAA AGG GGA TAT CAG-3′) before subcloning into pLNOH2-vaccine vector. All the new constructs were amplified without internal leader peptides and added 3′ to the V_H-leader included in pLNOH2 as described above. For

https://doi.org/10.4049/immunohorizons.1700038

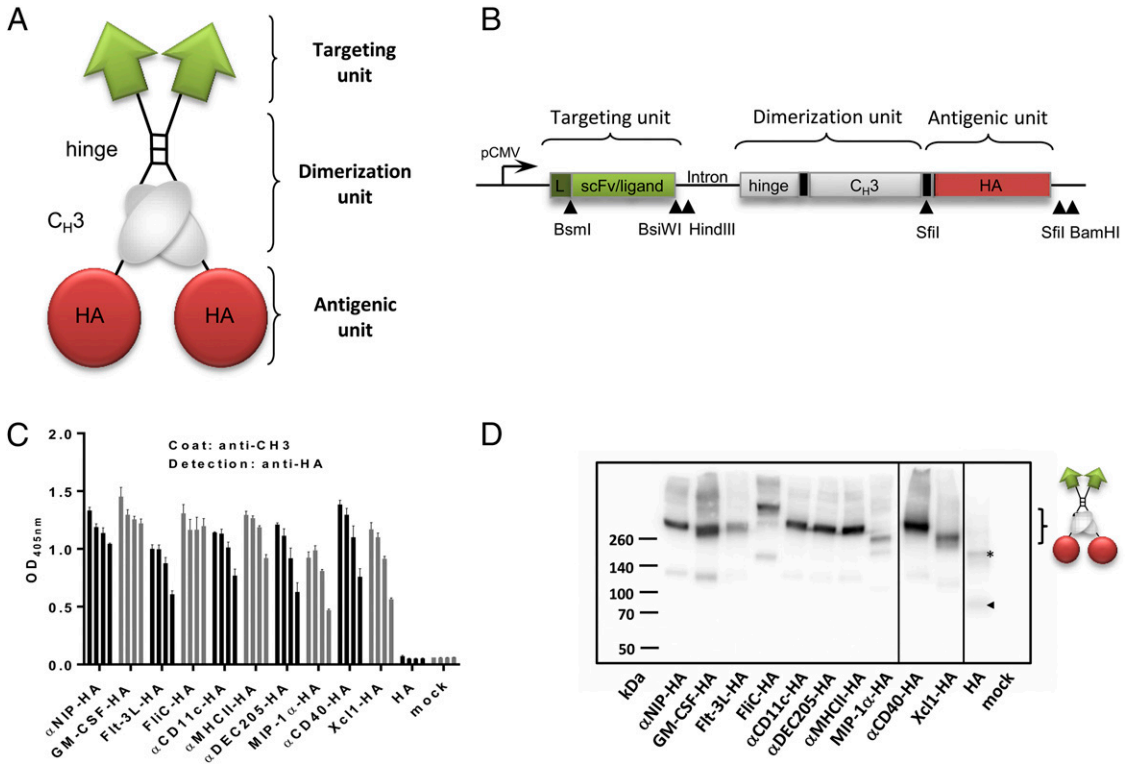

FIGURE 1. Targeted DNA vaccine constructs and characterization of encoded proteins.

(**A**) The dimeric vaccine protein structure consists of two identical chains, each with a targeting unit (green), a dimerization unit (gray), and an antigenic unit (red). The various vaccine constructs differ in the targeting unit but share the same dimerization unit (shortened hinge region and C_H3 of hγ3) and the same antigenic unit (HA) from the influenza virus A/Puerto Rico/8/34 (H1N1). (**B**) Overview of the DNA plasmid encoding the three units of the vaccine protein (A). Unique restriction enzyme sites for cloning are indicated. The plasmid contains a CMV promoter and a leader (L, dark green box). Short linkers (black boxes) increase the flexibility of the various units. (**C**) Vaccine proteins with the indicated targeting units in supernatants of transiently transfected HEK293E cells as measured by ELISA. Bars indicate supernatants diluted 1/1, 1/3, 1/9, and 1/27, respectively (mean ± SD). (**D**) Western blot under nonreducing conditions of supernatants from transiently transfected HEK293E cells developed with an HA-specific mAb. Homodimeric vaccine proteins are indicated by a bracket; the sizes are consistent with differences in sizes of the various targeting units. Putatively monomeric HA is indicated by an arrowhead, trimeric HA by an asterisk. The vertical lines indicate where parts of the image were joined.

anti-DEC205 and anti-CD11c, rearranged V(D)J genes from the H and L chain were PCR amplified from cDNA (First Strand cDNA Synthesis Kit; Amersham Biosciences) synthesized from mRNA extracted (Dynabeads mRNA DIRECT Purification Kit; Life Technologies) from the hybridoma NLDC-145 producing anti-DEC205 mAb (a kind gift from Prof. K. Kretschmer at Center for Regenerative Therapies, TU Dresden, Germany), and the N418 hybridoma (American Type Culture Collection) producing anti-CD11c. The primers were as follows: 5′V_L DEC205: 5′-GGT GTG CAT TCC GAC ATC CAG ATG ACA CAG TCT-3′, 3′V_L DEC205: 5′-GCC AGA GCC ACC TCC GCC AGA TCC GCC TCC ACC TTT CAA TTC CAG CTT GGT G-3′, 5′V_H DEC205: 5′-GGC GGA GGT GGC TCT GGC GGT GGC GGA TCG GAG GTG AAG CTG TTG GAA TCT-3′, and 3′V_H DEC205: 5′-GAC GTA CGA CTC ACC TGA GGA GAC TGT GAC CAT GAC-3′ for anti-DEC205 and 5′V_L CD11c: 5′-GGT GTG CAT TCC GAC ATC CAG ATG ACC CAG TCT-3′, 3′V_L CD11c: 5′-GCC AGA GCC ACC TCC GCC AGA TCC GCC TCC ACC TTT GAT TTC CAG CTT GGT G-3′, 5′V_H CD11c: 5′-GGC GGA GGT GGC TCT GGC GGT GGC GGA TCG GAG GTG CAG CTG GTG GAG AAG-3′, and 3′V_H CD11c: 5′-GAC GTA CGA CTC ACC TGA GGA GAC GGT GAC CTG GGT-3′ for anti-CD11c. The V_L and V_H PCR products were combined to a scFv format by PCR splicing by overlap extension and inserted into the targeting unit of the pLNOH2-vaccine vector. An internal BsmI site in $scFv^{anti\text{-}DEC205}$ was removed by quick change mutagenesis PCR (the primers used: 5′QBsmIVLDEC205: 5′-ACA AAA GTC AGG CAA TGC TCC TCAA-3′ and 3′QBsmIVLDEC205: 5′-TTG AGG AGC ATT GCC TGA CTT TTGT-3′) before subcloning into vaccine constructs with HA. The amino acid sequences of the scFvs are shown in Supplemental Fig. 1. The V_H and V_L used in $scFv^{anti\text{-}DEC205}$ correspond to the sequences for the DEC205-specific V_H and H_L found in GenBank AEP95114.1 and AEP95113.1, respectively. The nucleotide sequences will be provided upon request. Finally, the HA gene alone was ordered from GenScript including the signal peptide of H1PR8 (GenBank: EF467821.1). The Kozak site (5′-GCCACC ATG G-3′) was strengthened by mutating AAG into GAG right after ATG. The HA gene fragment was ordered with HindIII site 5′ to the signal peptide and BamHI

site 3′ following the stop codon TGA, thus allowing subcloning of HA alone into the pcDNA3.a vector (Invitrogen). All the various targeting units used in the targeted DNA constructs are listed in Table I.

Sequence alignment

The amino acid sequences of the scFvs derived from anti-DEC205 and anti-CD11c mAb were aligned and compared with the other scFvs used in this paper, using the ClustalW program (http://www.ch.embnet.org/software/ClustalW.html). The CDR loops were determined based on analysis by IMGT/V-QUEST (http://www.imgt.org/IMGT_vquest/vquest?livret=0&Option=mouseIg). A linker $(GGGGS)_3$ connects the V_L to V_H in that order.

In vitro analysis of the vaccine proteins by SDS-PAGE and Western blot analysis

Briefly, 1 μg of DNA in 50 μl OptiMEM (Life Technologies) and 2 μl Lipofectamine 2000 (Invitrogen) in 50 μl OptiMEM were mixed and incubated for 20 min at 25°C. The DNA/Lipofectamine solution was added to the HEK293E cells (1×10^5 per well in a 24-well plate), and incubated at 37°C in a 5% CO_2 humidified atmosphere. The medium was changed to the protein free cell medium FreeStyle 293 Expression Medium (Life Technologies by Life Technologies) the day after the transient transfection. Supernatants were collected after 3 d and centrifuged for 4 min at 13,000 rpm and up-concentrated 10 times with Vivaspin 20 Spin Columns 10 kDa cut off (Sartorius Stedim Biotech). The vaccine proteins were analyzed by SDS-PAGE using 4–12% Novex Tris-Glycine Gels (Invitrogen), with a Spectra Multicolor Broad Range Protein Ladder from Life Technologies, and developed with biotinylated HA-specific Abs (H-36-4-52, a kind gift from S. Weiss) and streptavidin-HRP (1:10 000; GE Healthcare) for 1 h at 25°C, before being developed with ECL Advance Western blotting Detection Kit (GE Healthcare) in a G:Box Chemi XX6 device (Syngene).

ELISAs for vaccine protein analysis

ELISAs were performed in Costar 96-well plates (Corning) coated with anti-human Cγ3 (1 μg/ml, MCA 878G; AbD Serotec), NIP-BSA (2.5 μg/ml), anti–mGM-CSF (1 μg/ml, 10236-08; AbD Serotec), rmCD40 fused to Fc (1 μg/ml, 1215-CD; R&D Systems) or anti–mFlt-3ligand (1 μg/ml, AF427; R&D Systems). Plates were blocked with PBS containing 1% BSA (25°C for 1 h). Supernatants from transiently transfected HEK293E cells (see above) were run in triplicate, serially diluted 3-fold in ELISA buffer (PBS containing 0.2% Tween and 0.1% BSA, 0.02% Na azide), and incubated for at least 1 h at 25°C. Biotinylated HA-specific Abs (1 μg/ml, H-36-4-52), anti-Xcl1 (1 μg/ml, LS-C16241; Lifespan Biosciences followed by anti-rabbit IgG-AP, 1:3000, from Sigma-Aldrich), biotinylated anti–MIP-1α (1 μg/ml, MAB415; R&D Systems), and biotinylated anti-FliC/Flagellin (1 μg/ml, ab193301; Abcam) were used to detect the respective vaccine constructs (45 min at 25°C). Biotinylated secondary reagents were followed by streptavidin-alkaline phosphatase (1:3000; GE Healthcare), and developed with addition of phosphatase substrate (1 mg/ml; Sigma-Aldrich) dissolved in substrate buffer. OD_{405} was measured with a TECAN Sunrise Microplate reader using the Magellan v5.03 program.

Flow cytometry for binding analysis of targeted vaccine proteins to APC

BALB/c splenocytes were FcγR blocked with medium containing 30% rat serum and 100 μg/ml 2.4G2 (anti-FcγRII/III Ab) for 20 min at 4°C. Supernatants from transiently transfected HEK293E cells were up-concentrated 10 times as described above, normalized by ELISA, and incubated with the splenocytes for 30 min at 4°C. A staining solution with FITC-conjugated anti-MHCII (I-A/I-E, rat IgG2a, 553623; BD Pharmingen) and anti-B220 allophycocyanin (anti-CD45R/B220 APC, rat IgG2a, 1665-11; SouthernBiotech), and matched isotype controls were used to gate $MHCII^+B220^-$ splenocytes for the binding analysis. Bound αCD11c- and αDEC205-targeted vaccine proteins were detected with biotinylated anti-human CH3 (2 μg/ml, HP6017; BD Pharmingen) followed by 2 μg/ml streptavidin-PE (BD Pharmingen). Staining incubations were for 10 min at 4°C followed by fixation with 2% paraformaldehyde. Cells were analyzed on a FACSCalibur (BD Biosciences) and the CellQuestPro software (BD Biosciences).

For preparation of Flt-3L–induced dendritic cells (DCs), bone marrow cells were harvested by flushing tibiae and femurs with medium. The cell suspension was filtered through a 70 μm Nylon cell strainer and seeded at a concentration of 2×10^6 cells per ml, 5 ml per well in a six-well plate. Then 0.1 μg/ml of Flt-3L (PeproTech, NJ) was added and the cells were incubated for 9 d at 37°C 5% CO_2 (21). Semiadherent cells were subsequently harvested and analyzed by flow cytometry. Conventional DC type 1 (cDC1) and cDC2 populations were gated based on staining with anti-CD45R/B220 (RA3-6B2; Tonbo Biosciences), anti-CD11c (N418; Tonbo Biosciences), anti-CD11b (M1/70; Tonbo Biosciences), and anti-CD24 (M1/69; BioLegend), and were analyzed for binding of GM-CSF-, Flt-3L- and FliC-targeted vaccine proteins as well as nontargeted αNIP control. In addition, the J774A.1 Mφ cell line was stained. Vaccine proteins and nontargeted controls were detected with biotinylated anti-HA mAb.

In vivo DNA vaccination and electroporation

Female BALB/c and C57BL/6 mice 6–8 wk of age were purchased from Taconic Farms, Denmark. Mice were anesthetized by a s.c. injection of Hypnorm/Dormicum (100 μl at 5 ml/kg) before each hind leg was shaved to prepare for vaccination. Plasmid DNA was purified using an Endofree-mega plasmid purification system (Qiagen). Next, 50 μl of 0.5 μg/μl DNA solved in sterile 0.9% NaCl solution (B. Braun) was injected i.m. into each quadriceps femoris muscle. Electroporation was performed immediately after injection with delivery of pulses from electrodes inserted i.m. flanking the injection site (Needle EP) by the Elgen electroporator device (Inovio Biomedical), as published in Liu et al. (22), with the electric pulses given as 5×60 ms at 50 V/400 mA and 200 ms delay. Blood samples were collected from the saphenous vein at regular intervals, spun down twice, and sera were frozen at −20°C.

ELISA for detection of Ag-specific Abs in sera from BALB/c and C57BL/6 mice

High-binding 96-well ELISA plates (CoStar) were coated with 2 μg/ml of inactivated PR8 influenza virus (Charles River

Laboratories). Serum samples were serially diluted (starting 1:50, dilution factor 1:3) in ELISA buffer. Abs in sera from BALB/c mice were detected with biotinylated anti-IgG (A2429; Sigma-Aldrich), anti-IgG1[a] (553599; BD Pharmingen), anti-IgG2a[a] (553502; BD Pharmingen). Sera from C57BL/6 mice were detected with biotinylated anti-IgG1[b] (553533; BD Pharmingen) and IgG2a[b] (IgG2c, 553504; BD Pharmingen). Otherwise, the serum ELISAs were run as described above for protein vaccine ELISAs. The Ab titer was defined as the highest dilution of a serum sample with OD values >(mean + 3SD) of NaCl-vaccinated mice. Samples with a titer <50 were given an endpoint titer of 1.

Influenza challenge of vaccinated mice

Vaccinated mice were challenged either 14 d or 9 mo (252 d) after a single vaccination i.m. as described above. Groups of anesthetized mice ($n = 10$ or 6 per group, respectively) were infected intranasally with 5xLD_{50} of PR8 influenza viruses in 20 μl (10 μl per nostril). LD_{50} of PR8 was determined as described before (13). Mice were monitored for weight loss and the humane endpoint was >20% weight loss, as required by the Norwegian Animal Research Authority.

Statistical analysis

All statistical analyses were performed using the GraphPad Prism version 7.02. Statistical differences between Ab titers and differences in % body weight at day 6 for various targeting groups were compared with Mann–Whitney two-tailed *t* test, nonparametric. Differences in survival were calculated by Mantel–Cox and differences in weight curves postinfection were calculated using two-way ANOVA. Correlations between weight day 6 and % survival or HA-specific total IgG/IgG1/IgG2a titer were analyzed using Pearson's correlation two-tailed test. A titer of 50 or more was considered a positive measurement. A p value ≤ 0.05 was considered statistically significant.

RESULTS

Targeted DNA vaccine constructs generate functional vaccine proteins in vitro

The targeted DNA vaccine constructs encode a homodimeric protein consisting of two identical chains, each composed of a targeting unit, a dimerization unit, and an antigenic unit (vaccibody, Fig. 1A) (8, 11). To directly compare the efficacy of the various targeting units, in the present experiments the dimerization and antigenic unit were kept unchanged in all constructs; respectively, a shortened hinge and Cγ3 domain from human IgG3 (dimerization unit), and the influenza Ag HA from influenza A virus [A/Puerto Rico/8/34 (H1N1), antigenic unit]. The HA was truncated at aa 18 and 541 to remove the leader peptide and the transmembrane regions (13). The DNA cassette with unique restriction enzymes sites (Fig. 1B) was used to insert the various targeting units. Five new targeting units were generated and tested together with four previously published targeting units. All constructs used are listed in Table I, including the nontargeted control αNIP-HA vaccine and HA alone. The latter was constructed with the intrinsic HA leader for proper expression (13). Most of the targeting units are expected to bind to surface molecules broadly expressed on various mouse DC subtypes (Table I). An exception is the Xcl1 targeting unit that binds uniquely to Xcr1 receptor found on $CD11c^+CD11b^-CD8\alpha^+$ cDC1, suggested to be highly efficient at cross-presenting Ag to $CD8^+$ T cells. Another exception is FliC, which recognizes TLR5 suggested to be expressed mainly on $CD11c^+CD11b^+CD8\alpha^-$ cDC2. However, TLR5 is also found on monocytes, neutrophils, and epithelial cells (Table I).

Prior to DNA vaccination, we tested if HEK293 cells transiently transfected with the plasmid vaccine constructs secreted proteins with anticipated structural features. ELISA analysis of vaccine proteins detected in supernatant by specific mAb confirmed proper folding of the Ag as well as the dimerization domain. All constructs were translated into vaccine proteins. The Flt-3L–HA and MIP-1α–HA plasmids were expressed in somewhat lower amounts compared with the others (Fig. 1C). The Western blot analysis developed by HA-specific Abs confirmed that all constructs were produced and expressed. The sizes were as expected, the various targeting units accounting for the size differences observed (Fig. 1D).

We next tested the functionality of the various targeting units expressed in vaccine proteins. Specific Abs recognized GM-CSF, Xcl1, MIP1α, FliC/flagellin, and Flt-3L in ELISAs (Fig. 2). The $scFv^{anti\text{-}NIP}$ in αNIP-HA bound to NIP-BSA, and $scFv^{anti\text{-}CD40}$ in αCD40-HA bound to rmCD40-Fc (Fig. 2A). The scFvs derived from the anti-DEC205 and anti-CD11c mAb were assembled as V_L–$(GGGGS)_3$ linker–V_H. The amino acid sequence for V_H in both $scFv^{anti\text{-}DEC205}$ and $scFv^{anti\text{-}CD11c}$ (Supplemental Fig. 1) have some discrepancies compared with the sequences published by others (7), but for the $scFv^{anti\text{-}DEC205}$ the corresponding sequences were found in GenBank AEP95114.1 and AEP95113.1. The αDEC205-HA and αCD11c-HA vaccine proteins bound $MHCII^+$ $B220^-$ splenocytes (Fig. 2B). GM-CSF–targeted vaccine protein bound Flt-3L–induced bone marrow cDC2, although weakly, and also the J774A.1 Mφ cell line. FliC-targeted vaccine protein bound Flt-3L–induced cDC2 as well as Mφ, as expected. The binding of Flt-3L–targeted vaccine was only detectable with the Mφ cell line and at very low levels (Fig. 2C). The latter result could indicate that the Flt-3L targeting moiety might not be functional. Arguing against this possibility, bat Flt-3L vaccibodies have previously been used for culturing bat bone marrow–derived mononuclear cells into Flt-3L–induced DC (23), suggesting that the Flt-3L–targeted vaccibody can bind to APCs. αMHCII (α$I\text{-}E^d$)-HA has previously been found to bind MHCII $I\text{-}E^d$–expressing cells (13, 18). MIP-1α and Xcl1 have also previously been shown to retain receptor binding and chemokine activity when used as targeting units in HA-containing vaccibodies (18, 19). Similarly, αCD40-targeted vaccine protein has been found to bind $CD19^+$ spleen cells from BALB/c mice (9). In conclusion, the various DNA vaccine constructs were all translated in vitro into targeting proteins with expected structures and specificities.

TABLE I. Overview of the various targeting units, short name vaccine constructs, receptors, and receptor-expressing cells

Targeting Unit	Short Name Vaccine Construct	Ligand	Ligand Expression on MPS Cells[a]	Other Receptor-Expressing Cells	Expression on DC Found in Skeletal Muscle (41)	Ref.
$scFv^{anti\text{-}NIP}$	αNIP-HA	None			None	
$GM\text{-}CSF^{b}$	GM-CSF-HA	GM-CSF receptor	cDC2, moDC, Mφ, LC	Neutrophils, eosinophils, and basophils	cDC2, moDC	(32, 53)
$Flt\text{-}3L^{b}$	Flt-3L-HA	Flt3 tyrosine kinase receptor	cDC1, cDC2, pDC	Hematopoietic stem and progenitor	cDC1, cDC2	(32, 54)
FliC/flagellin[c]	FliC-HA	TLR5	cDC2, Mφ	Neutrophils and epithelial	cDC2	(33, 55, 56)
$scFv^{anti\text{-}CD11c}$	αCD11c-HA	CD11c	cDC1, cDC2, pDC, moDC, LC, Mφ	Neutrophils	cDC1, cDC2, moDC	(32, 33)
$scFv^{anti\text{-}I\text{-}Ed}$	αMHCII-HA	I-E[d]	cDC1, cDC2, pDC, moDC, LC, Mφ	B	cDC1, cDC2, moDC	(32, 33, 57)
$scFv^{anti\text{-}DEC205}$	αDEC205-HA	CD205	cDC1, cDC2 (activated), LC DC[d], LC, Mφ	B and thymic epithelial	cDC1, cDC2 (activated) DC[d]	(32, 33, 58, 59)
$MIP\text{-}1\alpha^{b}$	MIP1α-HA	CCR1, 3 and 5		Eosinophils, basophils, NK, and T		(60)
$scFv^{anti\text{-}CD40}$	αCD40-HA	CD40	cDC1, cDC2, pDC, moDC, LC, Mφ	B, endothelial, and epithelials	cDC1, cDC2, moDC	(33)
$Xcl\text{-}1^{b}$	Xcl-1-HA	Xcr-1	cDC1		cDC1	(32, 33, 61)
None	HA	None			None	

[a]Ligand expression on cells of the mononuclear phagocyte system (MPS): cDC1, cDC2, plasmacytoid DC (pDC), Langerhans cells (LC), monocyte-derived DC (moDC), and Mφ, as defined by Guilliams et al. (32).
[b]Vaccine constructs include m variants of proteins.
[c]From *Salmonella typhimurium* phase 1 flagellar filament protein.
[d]DC subtype in mice not determined.

Targeted DNA vaccines induce HA-specific Abs of IgG1 and/or IgG2a subclasses

The efficacy of DNA vaccines at inducing HA-specific Abs was compared in vivo. Mice were vaccinated once with 25 μg DNA i.m. in each quadriceps, followed by electroporation to increase the uptake of DNA by muscle cells. Serum obtained 14 d after vaccination were analyzed for HA-specific IgG. We found that targeting by use of GM-CSF, FliC, αCD11c, αMHCII, αCD40, and Xcl1 all induced higher levels of total IgG than HA Ag alone, nontargeted αNIP, or sham vaccination (NaCl). However, only FliC, αCD11c, and αMHCII targeting induced significantly higher ($p < 0.05$) amounts of anti-HA Abs compared with the non-targeted αNIP-HA control (Fig. 3A).

When analyzing IgG subclasses induced by the various targeting specificities, GM-CSF, Flt-3L, FliC, αCD11c, and αMHCII induced higher HA-specific IgG1 titers than αNIP, but significance was only reached for FliC, αCD11c, and αMHCII (Fig. 3B). These three targeting moieties also induced high amounts of IgG2a. Other targeting moieties such as αCD40, Xcl1, and to some degree MIP-1α, induced IgG2a but little IgG1 (Fig. 3C). Overall, the FliC, αCD11c, αMHCII, and Xcl1 targeting units already showed a significant targeting effect 2 wk after one vaccination, suggesting they are particularly efficient at inducing HA-specific Abs at an early time point.

When plotting IgG1 versus IgG2a titers (Fig. 3D) and IgG1/IgG2a ratios (Fig. 3E), at least two groups could be discerned. One group consisting of MIP-1α-, αCD40-, and Xcl1-expressing vaccines preferentially induced IgG2a of significant titers. Another group consisting of FliC-, αCD11c-, and αMHCII-expressing vaccines induced both IgG1 and IgG2a of relatively high titers (Fig. 3D). GM-CSF-, Flit-3L-, and DEC205-expressing vaccines induced low amounts of IgG after 14 d.

The subclass profiles induced by the targeted DNA vaccines are maintained over prolonged periods of time

We next followed anti-HA Ab responses for 9 mo after a single i.m. vaccination. For reasons of clarity, only data for days 14, 56, and 252 are given in Fig. 4, whereas all data points are given in Supplemental Fig. 2. The data show that total IgG increased with time after immunization, with the hierarchical order: αMHCII > αCD11c > αCD40 > Xcl1 = MIP-1α > FliC > GM-CSF > Flt-3L > αDEC205.

Interestingly, whereas IgG2a titers increased with time, IgG1 titers declined after ~60 d (Supplemental Fig. 2). The targeting specificities that induced IgG2a > > IgG1 remained quite stable throughout the period with the following hierarchy: αCD40 > Xcl1 = MIP-1α > > DEC205 (blue group). As for targeting specificities inducing IgG1 > > IgG2a, represented by GM-CSF (orange group), comparatively small amounts of Abs were induced at all time periods. Concerning targeting specificities that elicited both IgG1 and IgG2a, the following order was observed: αMHCII > αCD11c > > FliC > > Flt-3L (green group). Taken together, the tendency seen on day 14 (Fig. 3) was generally perpetuated for 252 d (Fig. 4) with the exception that IgG1 responses declined after ~60 d.

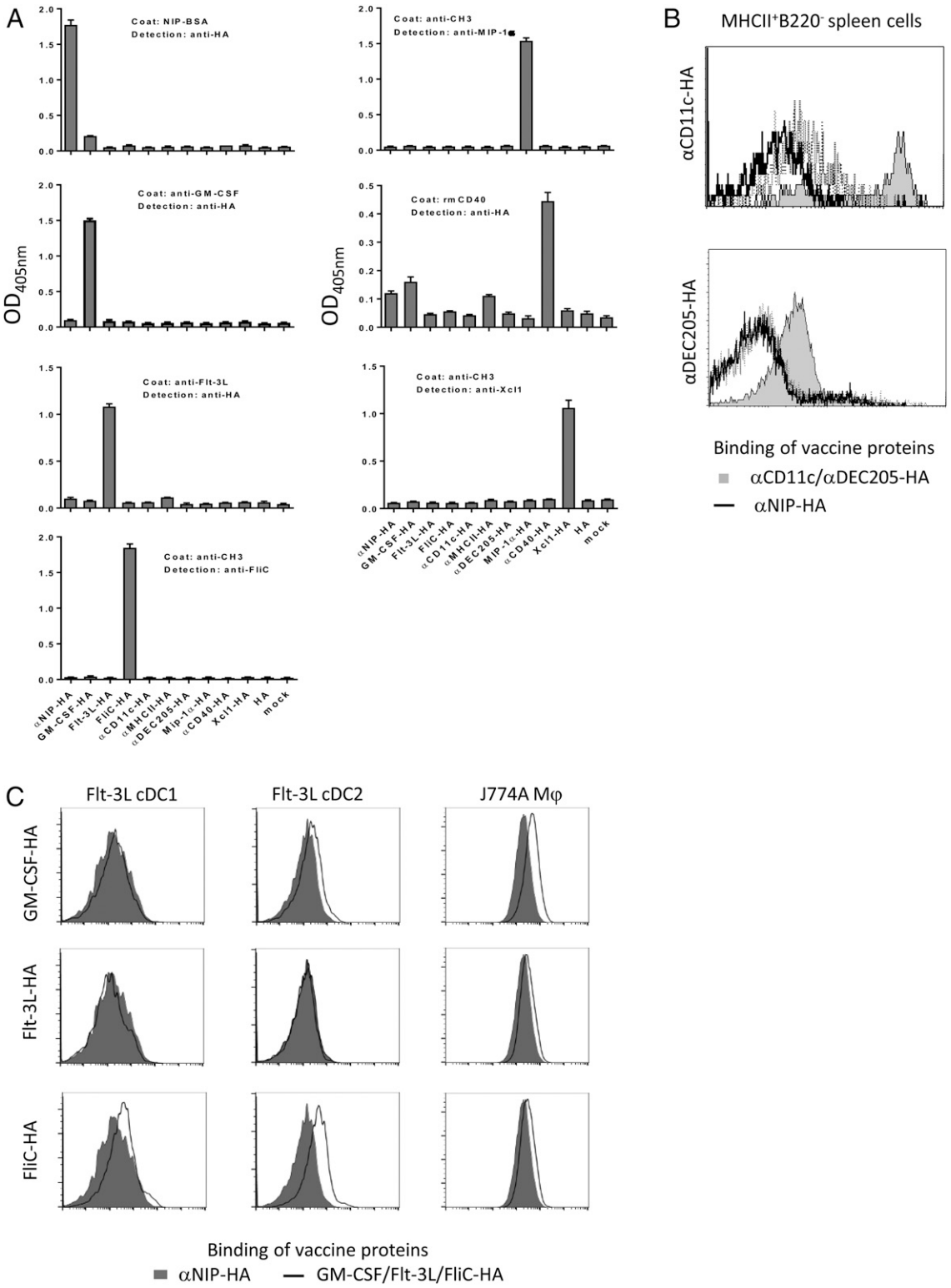

FIGURE 2. Characterization of the targeting units within the vaccine proteins.

(**A**) Supernatants from HEK293E cells transiently transfected with the various DNA plasmids were analyzed in sandwich ELISAs as indicated (mean ± SD). (**B**) Maintenance of CD11c and DEC205 specificity in targeted vaccine proteins. BALB/c splenocytes were stained with supernatants from HEK293E cells transiently transfected with αCD11c-HA or αDEC205-HA plasmids (gray) and gated $MHCII^{+}B220^{-}$ cells analyzed for binding of vaccine proteins. Isotype controls are shown as thick black lines, nonbinding αNIP-HA as a thin line, and mock control as a stippled lined. Bound proteins were detected with mAb that recognize $C_{\gamma}3$. (**C**) BM-derived Flt-3L DCs from BALB/c mice and the J774A Mφ cell line were **(Continued)**

IgG subclass–skewing is maintained upon immunization of Th1-prone C57BL/6 mice

We wanted to test if the IgG1 versus IgG2a responses were dependent on the targeted APC surface receptor and not due to Th2 proneness of BALB/c mice. C57BL/6 mice are Th1 prone. Therefore, FliC-, αCD11c-, Xcl1-targeted DNA vaccines as well as the nontargeted control were tested in C57BL/6 mice. The Xcl1-expressing vaccine induced mostly IgG2c in C57BL/6 mice, suggesting a Th1 profile, whereas αCD11c- and FliC-expressing vaccines induced IgG1 as well as IgG2c (Fig. 5). Thus, the IgG subclass–profiles observed in BALB/c mice appeared to be maintained in C57BL/6 mice. This suggests that the type of APC/cell surface receptor engaged by the vaccine overrides any influence of Th1 or Th2 proneness of mouse strains. For unknown reasons, αCD11c gave low responses in C57BL/6 compared with BALB/c. The αMHCII DNA vaccine could not be tested due to MHC polymorphisms between C57BL/6 and BALB/c.

Targeted DNA vaccines delivered once induce protection against PR8 influenza challenge

Because some of the targeting units induced high amounts of HA-specific Abs, we wanted to investigate if vaccination with the different targeting units could induce protection against a challenge with influenza A/PR/8/1934 (H1N1) virus (PR8). Briefly, 14 d after one i.m. vaccination, mice were challenged intranasally with $5xLD_{50}$ of PR8 virus and weight development monitored. Targeting with αMHCII induced full protection of the immunized mice whereas the αNIP-targeted or NaCl-vaccinated mice succumbed to infection, corresponding with previous results (13) (Fig. 6A). The various targeting groups were compared for weight at day 6 because that time point represents the nadir of the weight curves (Fig. 6A). Flt-3L, FliC, αCD11c, αMHCII, αCD40, and Xcl1 all induced significant protection compared with the αNIP-targeted vaccine (Fig. 6B). This result was confirmed upon analysis of survival (Supplemental Fig. 3). Of note, the mean weight on day 6 showed a significant correlation with the % survival of the various targeting groups (Fig. 6C), confirming that the mean weight on day 6 is predictive for protection.

Next, we evaluated the ability of the various targeting units to induce long-term protection in experiments where mice vaccinated once were challenged 9 mo later with influenza virus PR8 (Fig. 7). αMHCII-, MIP-1α-, and Xcl1-HA vaccines conferred significant resistance compared with nontargeted αNIP-HA (Fig. 7B, Supplemental Fig. 4). Again, there was a significant correlation between mean weight on day 6 and the % survival of the various targeting groups (Fig. 7C).

Protection correlated with HA-specific Abs

The levels of HA-specific total IgG, IgG1, and IgG2a Abs in sera from vaccinated mice were compared with the weights of the mice on day 6 after challenge. Anti-HA total IgG correlated significantly with % weight loss after influenza challenge in both the short term (14 d after vaccination, Fig. 8A) and long term (252 d after vaccination, Fig. 8B). When divided into IgG1 and IgG2a subclasses, a significant correlation was found for IgG1 and IgG2a after 14 d (Fig. 8A). However, only IgG2a titers displayed a significant correlation with weight loss after 252 d (Fig. 8B). These results demonstrate a significant correlation between amounts of anti-HA Abs and protection.

DISCUSSION

Targeted DNA vaccines work by making transfected cells secrete fusion proteins that target Ag to APC, resulting in enhanced Ab and T cell responses (6–9). In this study we show that targeting specificity greatly influences the quality of immune responses. Nine targeting specificities of DNA vaccines were compared, four of which have been previously published [MHCII (8, 13), CD40 (9), MIP-1α (11, 18), and Xcl1 (19)] and five new specificities (GM-CSF, Flt-3L, FliC, αCD11c, αDEC205). Readouts were the induction of Abs against the HA vaccine Ag and protection against an influenza virus challenge. The results show that targeted DNA vaccines significantly enhanced Ab responses in the following order: αMHCII > αCD11c > αCD40 > Xcl1 = MIP-1α> FliC > GM-CSF > Flt-3L > αDEC205. Moreover, the targeting specificity influenced the IgG subclass of Abs induced. Thus, GM-CSF induced IgG1 whereas Xcl1, MIP1-α, αCD40, and αDEC205 induced IgG2a. αMHCII, αCD11c, FliC, and Flt-3L induced mixed IgG1 and IgG2a Ab responses.

For logistic reasons, T cell responses were not measured in the current experiments. However, previous reports have shown that several of the targeting units used in this study (αMHCII, Xcl1, MIP1-α, αCD40) enhanced T cell responses (8, 9, 11, 13, 18, 19). Thus, the relatively selective IgG2a responses elicited by Xcl1, MIP-1α, and αCD40 targeting correlated with increased Th1 responses (9, 11, 18, 19), whereas the mixed IgG1/2a responses induced by αMHCII targeting was associated with a mixed Th1/2 profile (18, 24). Thus, for the novel specificities, it is likely that GM-CSF induces predominantly a Th2 response, αDEC205 a Th1 response, whereas αCD11c, FliC, and Flt-3L elicit a mixed Th1/2 response.

The IgG1 Abs appeared swiftly after a single vaccination, but declined from day 60. By comparison, the IgG2a responses occurred more slowly but lasted longer. The reason for this difference is unknown. Because a long duration of Ab production is a desired feature of vaccines, and IgG2a is endowed with potent biologic effector functions (25), targeting units that elicit IgG2a Abs appears advantageous. In addition, vaccine-induced IgG2a appears to be associated with Th1 responses (9, 11, 18, 19), which in itself could benefit protection against many infectious diseases.

analyzed for binding to vaccibody proteins by flow cytometry. DCs were defined as CD45R/B220$^-$CD11c$^+$ cells, and further split into CD11b$^+$ (cDC2) and CD24$^+$ (cDC1) populations, and evaluated for binding to GM-CSF–, Flt-3L–, and FliC-targeted vaccine proteins as compared with nontargeted αNIP-HA vaccines.

https://doi.org/10.4049/immunohorizons.1700038

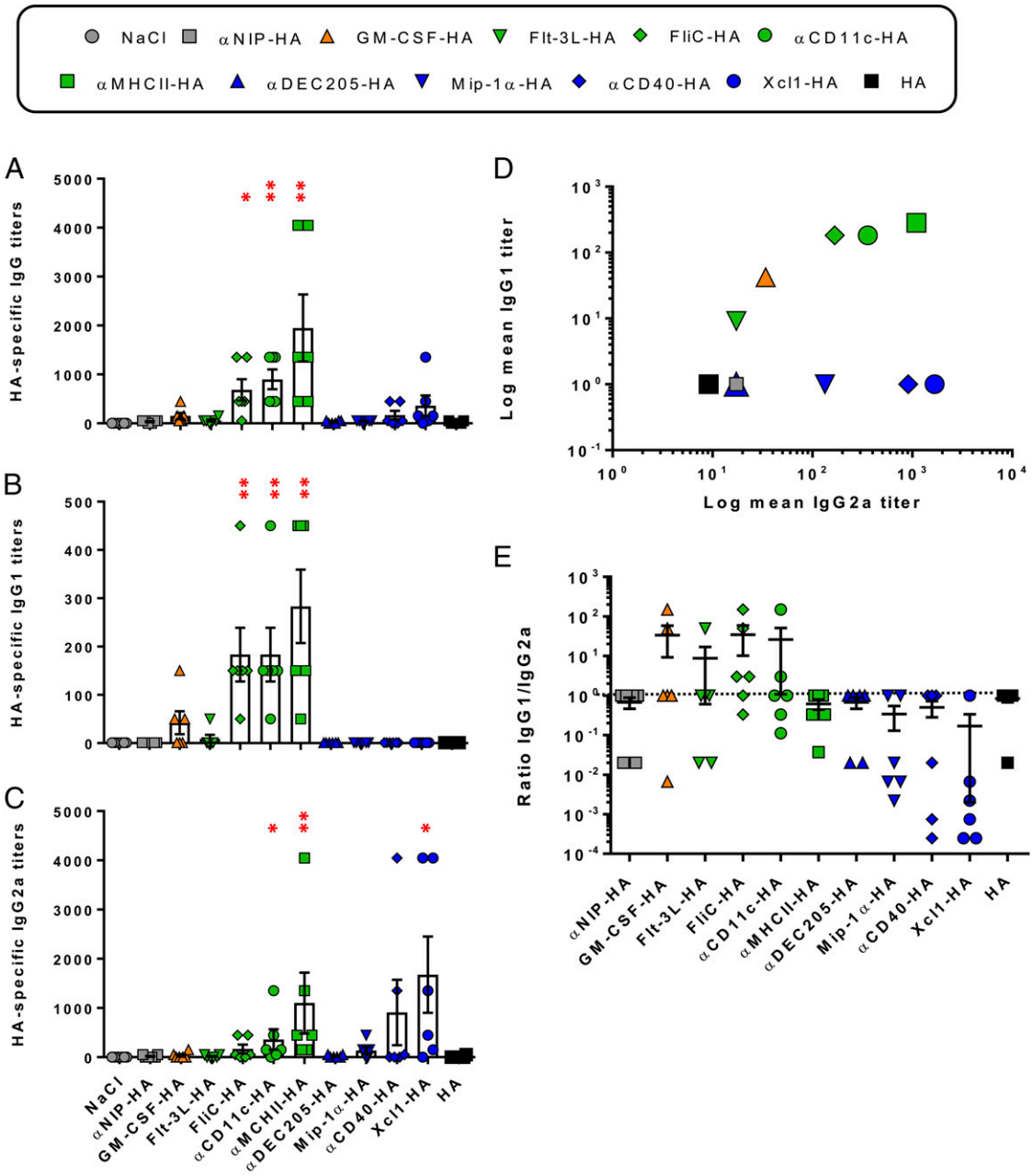

FIGURE 3. HA-specific Abs in serum 14 d after a single vaccination with the various targeted DNA vaccines.
Mice were vaccinated with 50 μl of 0.5 μg/μl DNA i.m. in each quadriceps, followed by electroporation of the injection site. Sera obtained 14 d later were analyzed for total IgG (**A**), IgG1 (**B**), and IgG2a (**C**) anti-HA Abs by ELISA ($n = 6$, bars indicate mean ± SEM, $*p < 0.05$, $**p < 0.01$ compared with the nontargeted αNIP-HA group by Mann–Whitney two-tailed t test). Samples with a titer <50 was given an endpoint titer of 1. (**D**) HA-specific IgG1 versus IgG2a titers were plotted for the various groups. For reasons of clarity, only means are shown. (**E**) HA-specific IgG1/IgG2a ratio shown for individual mice. Mean ± SEM is indicated. Dotted line indicates IgG1/IgG2a ratio = 1. Groups have been color coded as orange (primarily IgG1), blue (primarily IgG2a), or green (mix of IgG1 and IgG2a).

Why do targeted DNA vaccines enhance immune responses compared with nontargeted versions? First, targeted APC could enhance their presentation of antigenic peptides on MHCII molecules to $CD4^+$ T cells (26); such primed Th could later supply increased help to B cells. Secondly, targeted vaccine proteins could engender formation of APC–B cell synapses, as previously suggested by others (16) and us (10, 12). However, evidence of an APC–B cell synapse in vivo has not been firmly established. Supporting an APC–B cell synapse, αMHCII-HA vaccination resulted in preferential induction of Abs to the sialic acid binding

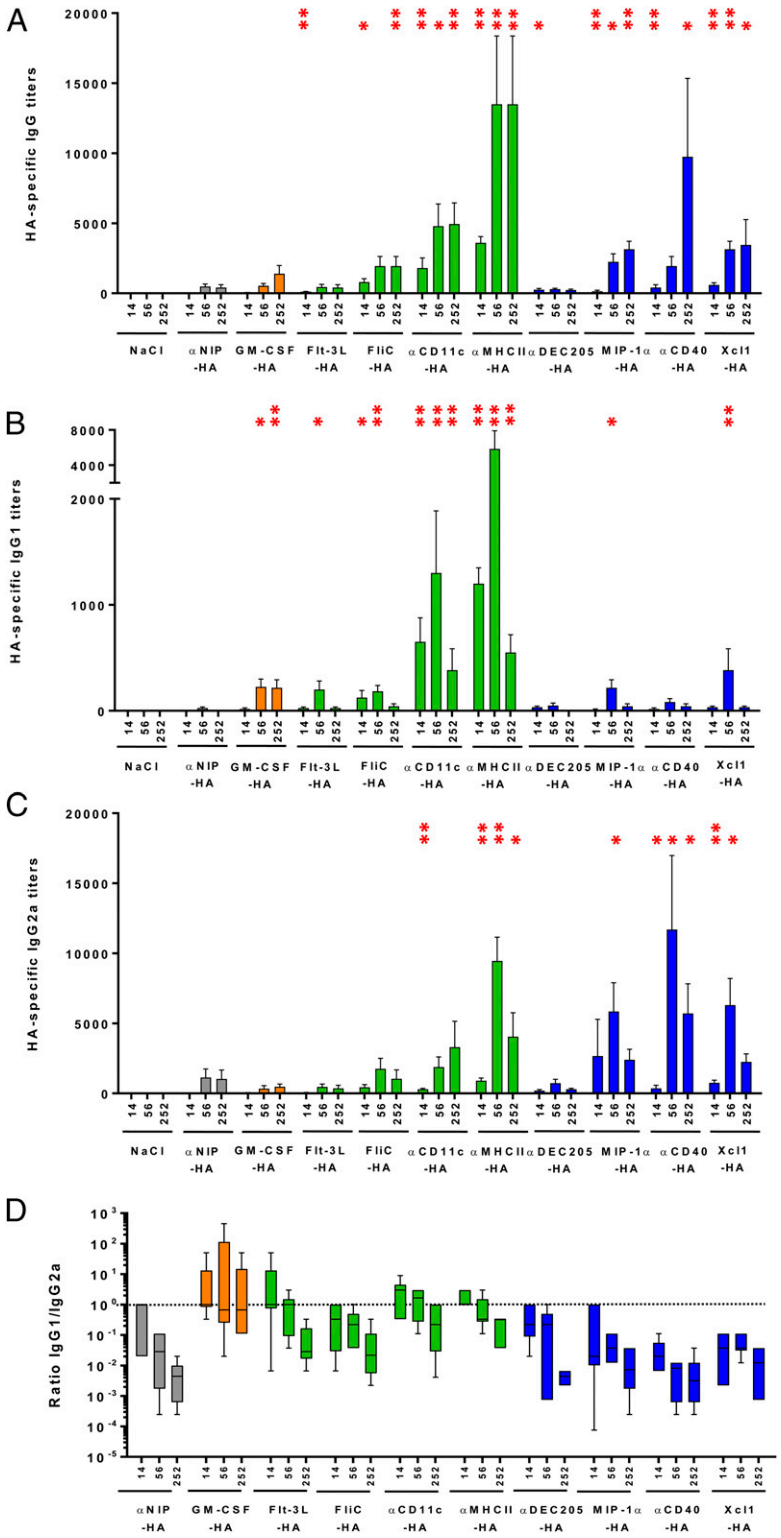

FIGURE 4. A single DNA vaccination induced prolonged Ab responses of IgG1 and/or IgG2a subclass.

Mice were vaccinated i.m. with 25 μg DNA in each quadriceps followed by electroporation. Serum obtained at day 14, 56, and 252 were analyzed for HA-specific total IgG (**A**), IgG1 (**B**), and IgG2a (**C**) for all the various targeted DNA vaccines (n = 6, mean ± SEM, *$p < 0.05$, **$p < 0.01$ compared with the nontargeted αNIP-HA group by Mann–Whitney two-tailed t test). (**D**) HA-specific IgG1/IgG2a ratio shown for individual mice on day 14, 56, and 252. Mean ± SEM is given. Dotted line indicates IgG1/IgG2a ratio = 1. Color coding as in Fig. 3.

https://doi.org/10.4049/immunohorizons.1700038

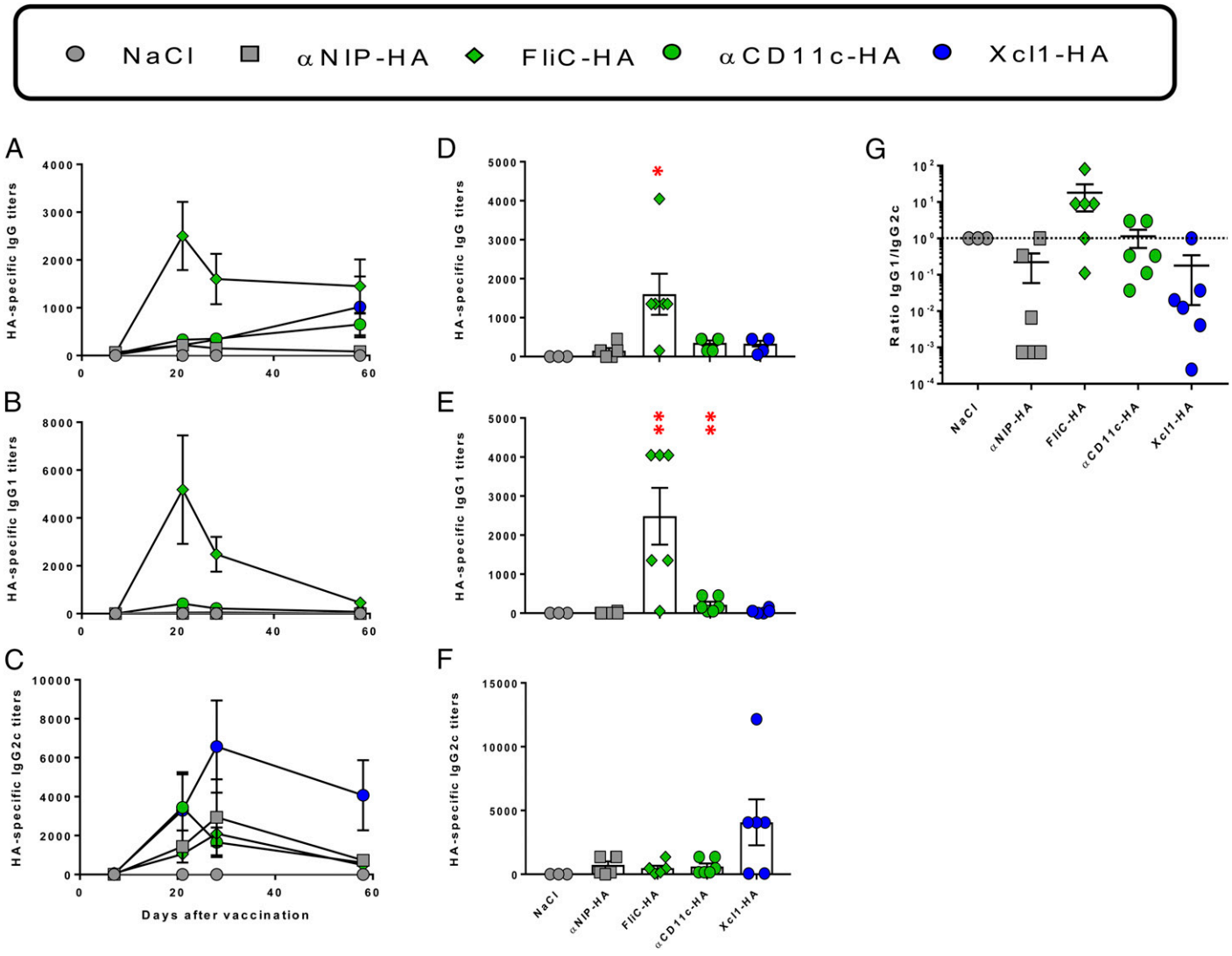

FIGURE 5. A single DNA vaccination of C57BL/6 mice induced Ab responses of IgG1 and/or IgG2c subclass.

Each mouse was vaccinated with 25 μg DNA i.m. in each quadriceps followed by electroporation of the injection site. Serum obtained at various time points were analyzed by ELISA for HA-specific total IgG (**A**), IgG1 (**B**), and IgG2c (**C**) for the indicated targeted DNA vaccines (n = 6, mean ± SEM). The individual titers for each mouse is shown for day 28 for total IgG (**D**), IgG1 (**E**), and IgG2c (**F**) anti-HA Abs by ELISA (n = 6, bars indicate mean ± SEM, *$p < 0.05$, **$p < 0.01$ compared with the nontargeted αNIP-HA group by Mann–Whitney two-tailed t test). Samples with titer <50 was given an endpoint titer of 1. (**G**) HA-specific IgG1/IgG2c ratio shown for individual mice. Mean ± SEM is indicated. Dotted line indicates IgG1/IgG2c ratio = 1.

site on the distal end of HA, consistent with the targeted vaccine protein bridging an APC–B cell synapse where the tip of HA points toward the BCR of B cells (13). Also supportive, vaccine proteins with a targeting unit that is poorly internalized resulted in enhanced Ab responses whereas T cell responses were reduced (21). In a putative APC–B cell synapse, the participant APC and B cell are likely to compete for endocytosis of the bridging vaccine protein. Depending on the outcome of such a tug of war, $CD4^+$ T cells may preferentially recognize MHCII-presented Ag on either the APC or the B cell, or both, possibly in three-cellular APC/B cell/T cell aggregates. APC–B cell synapses could occur in extra follicular areas in the cortex of lymph nodes, resulting in activated B cells that enter follicles and initiate germinal center formation (14–17).

The magnitude and isotype of vaccine-induced Ab responses could be influenced by the type of targeted APC, as well as the identity and density of the targeted cell surface molecule. The type of APC involved seems to play a role, thus, cDC1 appear to preferentially induce Th1 cells, whereas cDC2 primarily elicit Th2 cells (27). Supporting such a view, the selective induction of IgG2a and Th1 responses induced by Xcl1 vaccines [(19, 21), results in this study] could be due to the exclusive expression of the Xcr1

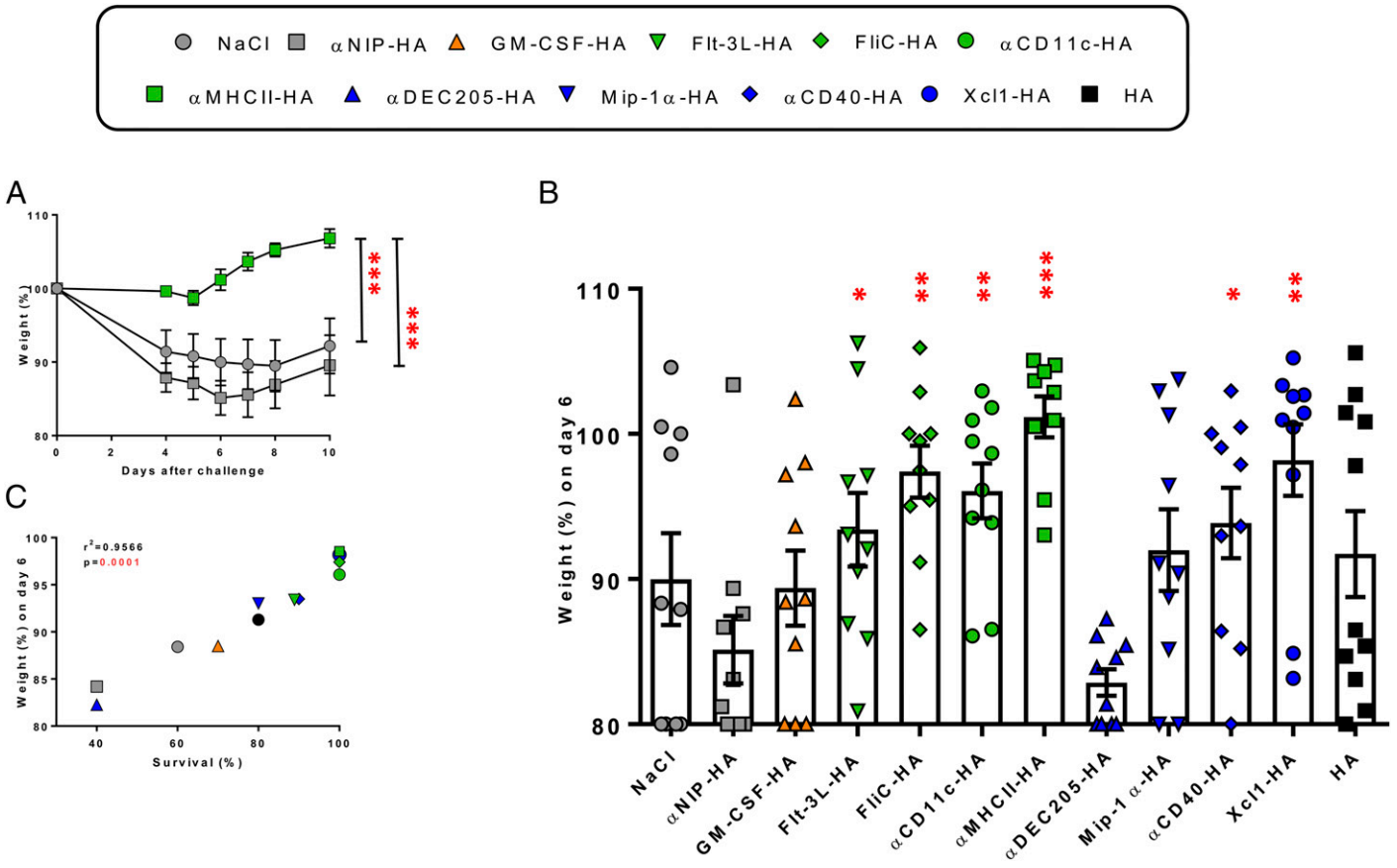

FIGURE 6. Targeted DNA vaccination induced protection against nasal challenge with influenza virus 14 d after DNA vaccination.
(**A**) Mice (n = 10 per group) were vaccinated with 25 μg DNA i.m. in each quadriceps and 14 d later challenged with 5xLD_{50} of influenza virus A (PR8/H1N1). Weight was monitored for 10 d as an indication of disease progression. Weight loss of 20% was defined as humane endpoint at which the mice were euthanized (*$p < 0.05$, **$p < 0.01$, ***$p < 0.001$, two-way ANOVA). For reasons of clarity only some groups are shown, see (**B**) for results of all groups. (B) Body weight (%) on day 6 for all the different groups. *$p < 0.05$, **$p < 0.01$, ***$p < 0.001$ compared with the nontargeted αNIP-HA group by Mann–Whitney two-tailed t test. (**C**) Mean weight on day 6 versus % survival after challenge with influenza A (PR8/H1N1). Correlation analyzed using Pearson correlation two-tailed test. Color coding as in Fig. 3.

receptor on cross-presenting cDC1 cells (28, 29). By contrast, αMHCII-vaccine proteins most likely target many different types of $MHCII^+$ APCs, perhaps explaining induction of a mixed IgG1/IgG2a response as well as a Th1/Th2 profile [(8, 13, 30), results in this study]. Similarly, αCD11c and Flt3 vaccine proteins should target both cDC1 and cDC2, contributing to the observed mixed IgG1/IgG2a responses (31–34). FliC-targeted vaccines induced a mixed IgG1 (early)/IgG2a (late) response. The IgG2a component was surprising because FliC binds TLR5 expressed by cDC2 (Fig. 2C) (35–38). However, FliC is also sensed by the NAIP5/NLRC4 (also known as IPAF) inflammasome (39, 40), which could contribute to the IgG2a response. It is more difficult to explain why αCD40 and MIP1-α preferentially induced IgG2a Abs, similar to Xcl1, because the surface molecules targeted by these vaccine proteins are expressed by many different types of APC (Table I). Further complicating the issues discussed above, the DNA vaccines of the current experiments were delivered i.m., and the types of targetable APC in skeletal muscle may be restricted compared with the body as a whole (41). Moreover, electroporation could influence APC composition due to its inflammatory effect (42, 43). Finally, vaccine proteins could drain as soluble molecules to lymph nodes, and target residential APC. Of note, results in BALB/c and C57BL/6 were similar, indicating that Th2-versus Th1-proneness of mice strains did not seriously influence the results.

The present results demonstrate that MHCII, CD11c, CD40, Xcr1, and CCR1/3/5 are the hitherto most promising targets because high Ab levels and protection against viral challenge were obtained with a single DNA immunization. Although T cells could contribute (13, 19), protection correlated with vaccine-induced ELISA Ab titers. Moreover, previous results demonstrated that vaccine-induced ELISA Ab titers correlated with levels of neutralizing Abs (13, 18, 19, 21). MHCII targeting in the present experiments resulted in the highest levels of long-lasting Abs, consistent with previous observations of us and others in rodents (8, 13, 44, 45). Recently, MHCII-targeted DNA vaccines were also shown to induce high titers of Abs in ferrets and pigs (30).

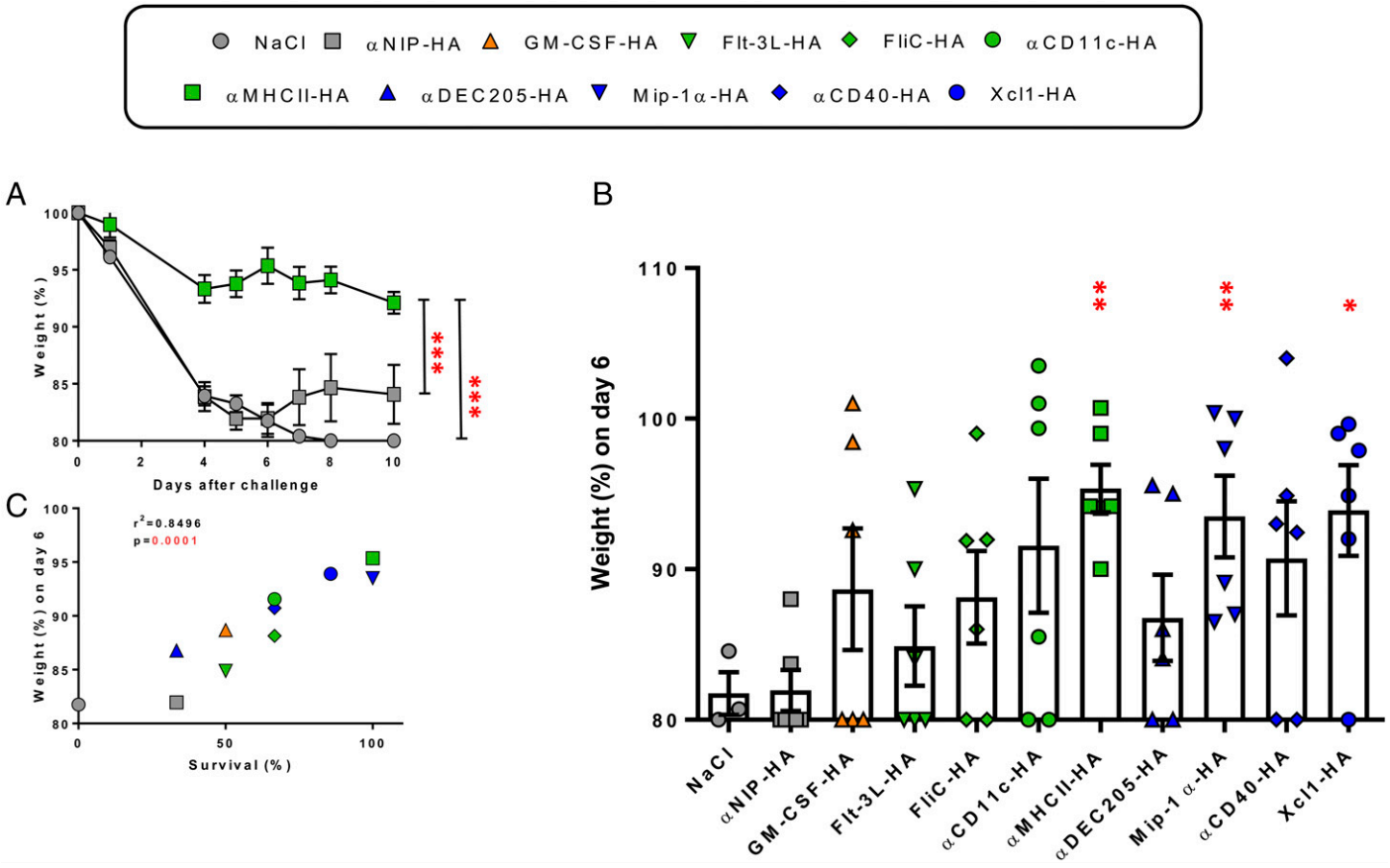

FIGURE 7. Long-lasting protection against nasal challenge with influenza virus 252 d after a single DNA vaccination.
(**A**) Mice were vaccinated i.m. with 25 μg DNA in each quadriceps and 252 d later challenged with 5xLD_{50} of influenza virus A (PR8/H1N1, $n = 6$ per group). Weight was monitored for 10 d. Weight loss of 20% was defined as humane endpoint (* $p < 0.05$, ** $p < 0.01$, *** $p < 0.001$, two-way ANOVA). For reasons of clarity only some groups are shown, see (**B**) for all groups. (B) The % body weight on day 6 for all the different groups. The results were analyzed with Mann–Whitney two-tailed t test, where * $p < 0.05$, ** $p < 0.01$, *** $p < 0.001$ compared with the nontargeted αNIP-HA vaccine. (**C**) Mean weight on day 6 versus % survival after challenge with influenza A (PR8/H1N1). Correlation analyzed using Pearson correlation two-tailed test. Color-coding as in Fig. 3.

CD11c-targeted DNA vaccination also induced relatively high titers of Abs, in agreement with previous results of others (31, 47). Xcl1, αCD40, and MIP-1α targeting induced delayed but persistent appearance of IgG2a Abs. These three targeting units induce potent Th1 (9, 11, 18, 19, 47) and CD8 (11, 18, 19, 47–49) responses that could have contributed to protection.

The IgG subclass of anti-HA Abs may be of special importance. Recently, broadly neutralizing HA stalk-specific Abs were found to require binding to FcγR for protection against influenza, and protection was restricted to the IgG2a subclass (50, 51). In contrast, neutralizing Abs that block the sialic acid–binding receptor of HA can equally well be of the IgG1 subclass (50). Thus, IgG1 and IgG2a anti-HA Abs observed in this study could both confer protection against influenza by partly overlapping mechanisms. In other infectious diseases, vaccines that preferentially elicit IgG2a Abs could be of special value due to the potent biologic effector functions associated with IgG2a such as complement fixation and Ab-dependent cellular cytotoxicity.

DNA vaccines are attractive because they are safe, and can be rapidly constructed and produced in large amounts. This is important in situations of pandemic threats, e.g., with avian influenza virus (52). Another advantage of DNA vaccines is their relative independence of a cold chain, due to the high resistance of DNA to degradation. This asset might be of particular importance for vaccinations in less developed areas of the world. A drawback is the generally low immune responses obtained with DNA vaccines in larger animals and humans (2). Immunogenicity may be increased by use of targeted DNA vaccines, as recently demonstrated in larger animals such as ferrets and pigs (30). However, for targeted DNA vaccines to be efficient, they need to be delivered with electroporation, which is hardly acceptable for prophylactic immunizations in humans. In this respect, it appears that electroporation might be replaced by a handheld needle-free device using high pressure air to introduce the DNA intradermally (jet delivery, PharmaJet). Thus, delivery of targeted DNA vaccines with either electroporation or jet delivery gave similar

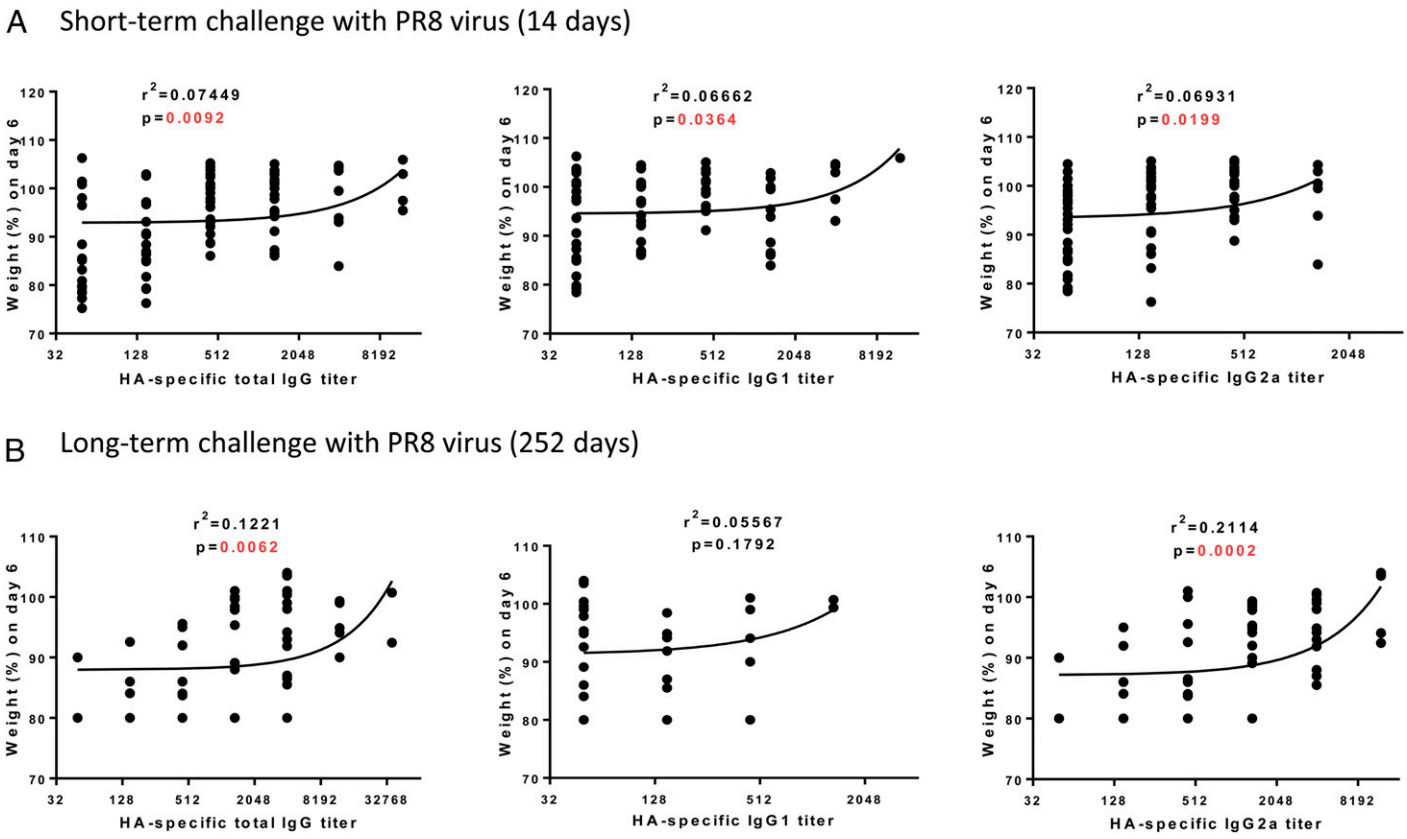

FIGURE 8. Protection against nasal challenge with influenza correlated both with IgG1 and IgG2a subclasses.
Mice were vaccinated once i.m. and challenged after 14 d (n = 10 per group) (**A**) or 252 d (n = 6 per group) with influenza PR8 (**B**). Total IgG, IgG1, and IgG2a titers in serum on the day before challenge were correlated with the % weight on day 6 after challenge. Mice with anti-HA titers ≥50, from all the groups of Figs. 3–6, were included in the analysis. The R square (r^2) and p values are shown in the figure. Significant p values are shown in red.

Ab responses in pigs (30). Importantly, jet delivery is essentially painless in pigs (30). Thus, prophylactic targeted DNA immunization in larger animals and humans should probably be combined with jet delivery rather than electroporation.

Promising targeting specificities defined in this study need not necessarily be the best. Thus, hundreds of other target specificities ought to be tested, which is challenging for logistical reasons. Such a task may be more easily carried out by use of targeted DNA vaccination than with purified fusion proteins. Because most vaccines owe their efficacy to the induction of Abs (1), screening of immunogenicity might be efficiently performed by measurement of specific Ig rather than labor-intensive T cell assays.

DISCLOSURES

B.B., R.B., A.B.F., E.F., and G.G. are inventors on patent applications filed on the vaccine molecules by the Technology Transfer Offices of the University of Oslo and Oslo University Hospital, according to institutional rules. B.B. is head of the scientific panel, and A.B.F. is Chief Science Officer of Vaccibody AS. They both hold shares in the company. The other authors have no financial conflicts of interest.

ACKNOWLEDGMENTS

We thank Elisabeth Vikse, Hilde Omholt, and Peter Hofgaard for expert technical assistance.

REFERENCES

1. Lambert, P. H., M. Liu, and C. A. Siegrist. 2005. Can successful vaccines teach us how to induce efficient protective immune responses? *Nat. Med.* 11(4 Suppl.): S54–S62.
2. Liu, M. A. 2011. DNA vaccines: an historical perspective and view to the future. *Immunol. Rev.* 239: 62–84.
3. Bergman, P. J., J. McKnight, A. Novosad, S. Charney, J. Farrelly, D. Craft, M. Wulderk, Y. Jeffers, M. Sadelain, A. E. Hohenhaus, et al. 2003. Long-term survival of dogs with advanced malignant melanoma after DNA vaccination with xenogeneic human tyrosinase: a phase I trial. *Clin. Cancer Res.* 9: 1284–1290.
4. Davis, B. S., G. J. Chang, B. Cropp, J. T. Roehrig, D. A. Martin, C. J. Mitchell, R. Bowen, and M. L. Bunning. 2001. West Nile virus recombinant DNA vaccine protects mouse and horse from virus challenge and expresses in vitro a noninfectious recombinant antigen that can be used in enzyme-linked immunosorbent assays. *J. Virol.* 75: 4040–4047.

https://doi.org/10.4049/immunohorizons.1700038

5. Li, L., F. Saade, and N. Petrovsky. 2012. The future of human DNA vaccines. *J. Biotechnol.* 162: 171–182.
6. Ruffini, P. A., A. Biragyn, M. Coscia, L. K. Harvey, S. C. Cha, B. Bogen, and L. W. Kwak. 2004. Genetic fusions with viral chemokines target delivery of nonimmunogenic antigen to trigger antitumor immunity independent of chemotaxis. *J. Leukoc. Biol.* 76: 77–85.
7. Demangel, C., J. Zhou, A. B. Choo, G. Shoebridge, G. M. Halliday, and W. J. Britton. 2005. Single chain antibody fragments for the selective targeting of antigens to dendritic cells. *Mol. Immunol.* 42: 979–985.
8. Fredriksen, A. B., I. Sandlie, and B. Bogen. 2006. DNA vaccines increase immunogenicity of idiotypic tumor antigen by targeting novel fusion proteins to antigen-presenting cells. *Mol. Ther.* 13: 776–785.
9. Schjetne, K. W., A. B. Fredriksen, and B. Bogen. 2007. Delivery of antigen to CD40 induces protective immune responses against tumors. *J. Immunol.* 178: 4169–4176.
10. Grødeland, G., and B. Bogen. 2015. Efficient vaccine against pandemic influenza: combining DNA vaccination and targeted delivery to MHC class II molecules. *Expert Rev. Vaccines* 14: 805–814.
11. Fredriksen, A. B., and B. Bogen. 2007. Chemokine-idiotype fusion DNA vaccines are potentiated by bivalency and xenogeneic sequences. *Blood* 110: 1797–1805.
12. Fredriksen, A. B., I. Sandlie, and B. Bogen. 2012. Targeted DNA vaccines for enhanced induction of idiotype-specific B and T cells. *Front. Oncol.* 2: 154.
13. Grodeland, G., S. Mjaaland, K. H. Roux, A. B. Fredriksen, and B. Bogen. 2013. DNA vaccine that targets hemagglutinin to MHC class II molecules rapidly induces antibody-mediated protection against influenza. *J. Immunol.* 191: 3221–3231.
14. Wykes, M., A. Pombo, C. Jenkins, and G. G. MacPherson. 1998. Dendritic cells interact directly with naive B lymphocytes to transfer antigen and initiate class switching in a primary T-dependent response. *J. Immunol.* 161: 1313–1319.
15. Qi, H., J. G. Egen, A. Y. Huang, and R. N. Germain. 2006. Extrafollicular activation of lymph node B cells by antigen-bearing dendritic cells. *Science* 312: 1672–1676.
16. Batista, F. D., D. Iber, and M. S. Neuberger. 2001. B cells acquire antigen from target cells after synapse formation. *Nature* 411: 489–494.
17. Lindquist, R. L., G. Shakhar, D. Dudziak, H. Wardemann, T. Eisenreich, M. L. Dustin, and M. C. Nussenzweig. 2004. Visualizing dendritic cell networks in vivo. *Nat. Immunol.* 5: 1243–1250.
18. Grødeland, G., S. Mjaaland, G. Tunheim, A. B. Fredriksen, and B. Bogen. 2013. The specificity of targeted vaccines for APC surface molecules influences the immune response phenotype. *PLoS One* 8: e80008.
19. Fossum, E., G. Grødeland, D. Terhorst, A. A. Tveita, E. Vikse, S. Mjaaland, S. Henri, B. Malissen, and B. Bogen. 2015. Vaccine molecules targeting Xcr1 on cross-presenting DCs induce protective CD8 + T-cell responses against influenza virus. *Eur. J. Immunol.* 45: 624–635.
20. Norderhaug, L., T. Olafsen, T. E. Michaelsen, and I. Sandlie. 1997. Versatile vectors for transient and stable expression of recombinant antibody molecules in mammalian cells. *J. Immunol. Methods* 204: 77–87.
21. Gudjonsson, A., A. Lysén, S. Balan, V. Sundvold-Gjerstad, C. Arnold-Schrauf, L. Richter, E. S. Bækkevold, M. Dalod, B. Bogen, and E. Fossum. 2017. Targeting influenza virus hemagglutinin to Xcr1+ dendritic cells in the absence of receptor-mediated endocytosis enhances protective antibody responses. *J. Immunol.* 198: 2785–2795.
22. Liu, J., R. Kjeken, I. Mathiesen, and D. H. Barouch. 2008. Recruitment of antigen-presenting cells to the site of inoculation and augmentation of human immunodeficiency virus type 1 DNA vaccine immunogenicity by in vivo electroporation. *J. Virol.* 82: 5643–5649.
23. Zhou, P., Y. T. Chionh, S. E. Irac, M. Ahn, J. H. Jia Ng, E. Fossum, B. Bogen, F. Ginhoux, A. T. Irving, C. A. Dutertre, and L. F. Wang. 2016. Unlocking bat immunology: establishment of Pteropus alecto bone marrow-derived dendritic cells and macrophages. *Sci. Rep.* 6: 38597.
24. Grødeland, G., E. Fossum, and B. Bogen. 2015. Polarizing T and B cell responses by APC-targeted subunit vaccines. *Front. Immunol.* 6: 367.
25. Nimmerjahn, F., P. Bruhns, K. Horiuchi, and J. V. Ravetch. 2005. FcgammaRIV: a novel FcR with distinct IgG subclass specificity. *Immunity* 23: 41–51.
26. Lunde, E., K. H. Western, I. B. Rasmussen, I. Sandlie, and B. Bogen. 2002. Efficient delivery of T cell epitopes to APC by use of MHC class II-specific Troybodies. *J. Immunol.* 168: 2154–2162.
27. Moser, M., and K. M. Murphy. 2000. Dendritic cell regulation of TH1-TH2 development. *Nat. Immunol.* 1: 199–205 .
28. Dorner, B. G., M. B. Dorner, X. Zhou, C. Opitz, A. Mora, S. Güttler, A. Hutloff, H. W. Mages, K. Ranke, M. Schaefer, et al. 2009. Selective expression of the chemokine receptor XCR1 on cross-presenting dendritic cells determines cooperation with CD8+ T cells. *Immunity* 31: 823–833.
29. Crozat, K., S. Tamoutounour, T. P. Vu Manh, E. Fossum, H. Luche, L. Ardouin, M. Guilliams, H. Azukizawa, B. Bogen, B. Malissen, et al. 2011. Cutting edge: expression of XCR1 defines mouse lymphoid-tissue resident and migratory dendritic cells of the CD8α+ type. *J. Immunol.* 187: 4411–4415.
30. Grodeland, G., A. B. Fredriksen, G. A. Løset, E. Vikse, L. Fugger, and B. Bogen. 2016. Antigen targeting to human HLA class II molecules increases efficacy of DNA vaccination. *J. Immunol.* 197: 3575–3585.
31. White, A. L., A. L. Tutt, S. James, K. A. Wilkinson, F. V. Castro, S. V. Dixon, J. Hitchcock, M. Khan, A. Al-Shamkhani, A. F. Cunningham, and M. J. Glennie. 2010. Ligation of CD11c during vaccination promotes germinal centre induction and robust humoral responses without adjuvant. *Immunology* 131: 141–151.
32. Guilliams, M., F. Ginhoux, C. Jakubzick, S. H. Naik, N. Onai, B. U. Schraml, E. Segura, R. Tussiwand, and S. Yona. 2014. Dendritic cells, monocytes and macrophages: a unified nomenclature based on ontogeny. *Nat. Rev. Immunol.* 14: 571–578.
33. Cohn, L., and L. Delamarre. 2014. Dendritic cell-targeted vaccines. *Front. Immunol.* 5: 255.
34. Matthews, W., C. T. Jordan, M. Gavin, N. A. Jenkins, N. G. Copeland, and I. R. Lemischka. 1991. A receptor tyrosine kinase cDNA isolated from a population of enriched primitive hematopoietic cells and exhibiting close genetic linkage to c-kit. *Proc. Natl. Acad. Sci. USA* 88: 9026–9030.
35. Hayashi, F., K. D. Smith, A. Ozinsky, T. R. Hawn, E. C. Yi, D. R. Goodlett, J. K. Eng, S. Akira, D. M. Underhill, and A. Aderem. 2001. The innate immune response to bacterial flagellin is mediated by Toll-like receptor 5. *Nature* 410: 1099–1103.
36. Robbins, S. H., T. Walzer, D. Dembélé, C. Thibault, A. Defays, G. Bessou, H. Xu, E. Vivier, M. Sellars, P. Pierre, et al. 2008. Novel insights into the relationships between dendritic cell subsets in human and mouse revealed by genome-wide expression profiling. *Genome Biol.* 9: R17.
37. Liu, G., L. Song, L. Reiserova, U. Trivedi, H. Li, X. Liu, D. Noah, F. Hou, B. Weaver, and L. Tussey. 2012. Flagellin-HA vaccines protect ferrets and mice against H5N1 highly pathogenic avian influenza virus (HPAIV) infections. *Vaccine* 30: 6833–6838.
38. Song, L., G. Liu, S. Umlauf, X. Liu, H. Li, H. Tian, L. Reiserova, F. Hou, R. Bell, and L. Tussey. 2014. A rationally designed form of the TLR5 agonist, flagellin, supports superior immunogenicity of Influenza B globular head vaccines. *Vaccine* 32: 4317–4323.
39. Franchi, L., A. Amer, M. Body-Malapel, T. D. Kanneganti, N. Ozören, R. Jagirdar, N. Inohara, P. Vandenabeele, J. Bertin, A. Coyle, et al. 2006. Cytosolic flagellin requires Ipaf for activation of caspase-1 and interleukin 1beta in *Salmonella*-infected macrophages. *Nat. Immunol.* 7: 576–582.
40. Lin, K. H., L. S. Chang, C. Y. Tian, Y. C. Yeh, Y. J. Chen, T. H. Chuang, S. J. Liu, and C. H. Leng. 2016. Carboxyl-terminal

fusion of E7 into Flagellin shifts TLR5 activation to NLRC4/NAIP5 activation and induces TLR5-independent anti-tumor immunity. *Sci. Rep.* 6: 24199.
41. Langlet, C., S. Tamoutounour, S. Henri, H. Luche, L. Ardouin, C. Grégoire, B. Malissen, and M. Guilliams. 2012. CD64 expression distinguishes monocyte-derived and conventional dendritic cells and reveals their distinct role during intramuscular immunization. *J. Immunol.* 188: 1751–1760.
42. Løvås, T. O., J. C. Bruusgaard, I. Øynebråten, K. Gundersen, and B. Bogen. 2014. DNA vaccines: MHC II-targeted vaccine protein produced by transfected muscle fibres induces a local inflammatory cell infiltrate in mice. *PLoS One* 9: e108069.
43. Peng, B., Y. Zhao, L. Xu, and Y. Xu. 2007. Electric pulses applied prior to intramuscular DNA vaccination greatly improve the vaccine immunogenicity. *Vaccine* 25: 2064–2073.
44. Carayanniotis, G., and B. H. Barber. 1987. Adjuvant-free IgG responses induced with antigen coupled to antibodies against class II MHC. *Nature* 327: 59–61.
45. Snider, D. P., and D. M. Segal. 1987. Targeted antigen presentation using crosslinked antibody heteroaggregates. *J. Immunol.* 139: 1609–1616.
46. Skea, D. L., and B. H. Barber. 1993. Studies of the adjuvant-independent antibody response to immunotargeting. Target structure dependence, isotype distribution, and induction of long term memory. *J. Immunol.* 151: 3557–3568.
47. Yin, W., L. Gorvel, S. Zurawski, D. Li, L. Ni, D. Duluc, K. Upchurch, J. Kim, C. Gu, R. Ouedraogo, et al. 2016. Functional specialty of CD40 and dendritic cell surface lectins for exogenous antigen presentation to CD8(+) and CD4(+) T cells. *EBioMedicine* 5: 46–58.
48. Hartung, E., M. Becker, A. Bachem, N. Reeg, A. Jäkel, A. Hutloff, H. Weber, C. Weise, C. Giesecke, V. Henn, et al. 2015. Induction of potent CD8 T cell cytotoxicity by specific targeting of antigen to cross-presenting dendritic cells in vivo via murine or human XCR1. *J. Immunol.* 194: 1069–1079.
49. Terhorst, D., E. Fossum, A. Baranska, S. Tamoutounour, C. Malosse, M. Garbani, R. Braun, E. Lechat, R. Crameri, B. Bogen, et al. 2015. Laser-assisted intradermal delivery of adjuvant-free vaccines targeting XCR1+ dendritic cells induces potent antitumoral responses. *J. Immunol.* 194: 5895–5902.
50. DiLillo, D. J., G. S. Tan, P. Palese, and J. V. Ravetch. 2014. Broadly neutralizing hemagglutinin stalk-specific antibodies require FcγR interactions for protection against influenza virus in vivo. *Nat. Med.* 20: 143–151.
51. Schmitz, N., R. R. Beerli, M. Bauer, A. Jegerlehner, K. Dietmeier, M. Maudrich, P. Pumpens, P. Saudan, and M. F. Bachmann. 2012. Universal vaccine against influenza virus: linking TLR signaling to anti-viral protection. *Eur. J. Immunol.* 42: 863–869.
52. Andersen, T. K., F. Zhou, R. Cox, B. Bogen, and G. Grødeland. 2017. A DNA vaccine that targets hemagglutinin to antigen-presenting cells protects mice against H7 influenza. *J. Virol.* DOI: 10.1128/JVI.01340-17.
53. Guthridge, M. A., F. C. Stomski, D. Thomas, J. M. Woodcock, C. J. Bagley, M. C. Berndt, and A. F. Lopez. 1998. Mechanism of activation of the GM-CSF, IL-3, and IL-5 family of receptors. *Stem Cells* 16: 301–313.
54. Matthews, W., C. T. Jordan, G. W. Wiegand, D. Pardoll, and I. R. Lemischka. 1991. A receptor tyrosine kinase specific to hematopoietic stem and progenitor cell-enriched populations. *Cell* 65: 1143–1152.
55. Shibata, T., N. Takemura, Y. Motoi, Y. Goto, T. Karuppuchamy, K. Izawa, X. Li, S. Akashi-Takamura, N. Tanimura, J. Kunisawa, et al. 2012. PRAT4A-dependent expression of cell surface TLR5 on neutrophils, classical monocytes and dendritic cells. *Int. Immunol.* 24: 613–623.
56. Gewirtz, A. T., T. A. Navas, S. Lyons, P. J. Godowski, and J. L. Madara. 2001. Cutting edge: bacterial flagellin activates basolaterally expressed TLR5 to induce epithelial proinflammatory gene expression. *J. Immunol.* 167: 1882–1885.
57. Ting, J.P.-Y., and J. Trowsdale. 2002. Genetic control of MHC class II expression. *Cell* 109: S21–S33.
58. Inaba, K., W. J. Swiggard, M. Inaba, J. Meltzer, A. Mirza, T. Sasagawa, M. C. Nussenzweig, and R. M. Steinman. 1995. Tissue distribution of the DEC-205 protein that is detected by the monoclonal antibody NLDC-145. I. Expression on dendritic cells and other subsets of mouse leukocytes. *Cell. Immunol.* 163: 148–156.
59. Witmer-Pack, M. D., W. J. Swiggard, A. Mirza, K. Inaba, and R. M. Steinman. 1995. Tissue distribution of the DEC-205 protein that is detected by the monoclonal antibody NLDC-145. II. Expression in situ in lymphoid and nonlymphoid tissues. *Cell. Immunol.* 163: 157–162.
60. Menten, P., A. Wuyts, and J. Van Damme. 2002. Macrophage inflammatory protein-1. *Cytokine Growth Factor Rev.* 13: 455–481.
61. Crozat, K., R. Guiton, V. Contreras, V. Feuillet, C. A. Dutertre, E. Ventre, T.-P. Vu Manh, T. Baranek, A. K. Storset, J. Marvel, et al. 2010. The XC chemokine receptor 1 is a conserved selective marker of mammalian cells homologous to mouse CD8α$^+$ dendritic cells. *J. Exp. Med.* 207: 1283–1292.

```
                                        CDR1                                CDR2
αCD11c      DIQMTQSPSSLPASLGDRVTIHCQASQDISN----YLTWYQQKPGKAPKLLIYETNKLAD
αDEC205     DIQMTQSPSFLSTSLGNSITITCHASQNIKG----WLAWYQQKSGNAPQLLIYKASSLQS
αCD40       DTVLTQSP-ALAVSPGERVTISCRASDSVST----LMHWYQQKPGQQPKLLIYLASHLES
αMHCII      QVQLTQSPASLAVSLGQRATISCRASKSVSTSGYSYMHWYQQKPGQPPKLLIYLTSNLES
αNIP        QAVVTQES-ALTTSPGETVTLTCRSSTGAVTTSN-YANWVQEKPDHLFTGLIGGTNNRAP

                                                CDR3                Linker
αCD11c      GVPSRFSGSGSGRDYSFTISSLESEDVGSYYCQHYYDYPRTFGPGTKLEIKGGGGSGGGG
αDEC205     GVPSRFSGSGSGTDYIFTISNLQPEDIATYYCQHYQSFPWTFGGGTKLELKGGGGSGGGG
αCD40       GVPARFSGSGSGTDFTLTIDPVEADDTATYYCQQSWNDPWTFGGGTKLELKGGGGSGGGG
αMHCII      GVPARFSGSGSGTDFTLNIHPVEEEDAATYYCQHSRELPWTFGGGTKLEIKGGGGSGGGG
αNIP        GVPARFSGSLIGDKAALTITGTQTEDEAMYFCALWYSNHWVFGGGTKLTVLGGGGSGGGG

                                        CDR1                        CDR2
αCD11c      SGGGGSEVQLVEKGGGLVQPGKSLKLSCAASGFTFSEYWMNWVRQAPGKGLEWVGVIKYK
αDEC205     SGGGGSEVKLLESGGGLVQPGGSLRLSCAASGFTFNDFYMNWIRQPPGQAPEWLGVIRNK
αCD40       SGGGGSEVQLVESDGGLVQPGRSLKLPCAASGFTFSDYYMAWVRQAPTKGLEWVASISYD
αMHCII      SGGGGSQVQLQQSGPDLVKPGASVTISCKASGYAFSSSWMSWLKQRPGKGLEWIGWIFPR
αNIP        SGGGGSQVQLQQPGAELVKPGASVKLSCKASGYTFTSYWMHWVKQRPGRGLEWIGRIDPN

                                                CDR3
αCD11c      YSNYATEYAESVKGRFTISRDDSKSSVYLQMNNLRAEDTAIYYCARTWENWYFD----FW
αDEC205     GNGYTTEVNTSVKGRFTISRDNTQNILYLQMNSLRAEDTAIYYCARGGPYYYSGDDAPYW
αCD40       GS--STYYRDSVKGRFTISRDNAKSTLYLQMDSLRSEDTATYYCGR--HSSYFD----YW
αMHCII      DG--DTNYNGKFKGKATLTADKSSSTAYMQLSSLTSEDSAVYFCARRGDYHYGMD---YW
αNIP        SG--GTKYNEKFKSKATLTVDKPSSTAYMQLSSLTSEDSAVYYCAR--YDYYGSSYFDYW


αCD11c      GQGTQVTVSS
αDEC205     GQGVMVTVSS
αCD40       GQGVMVTVSS
αMHCII      GQGTSVTVSS
αNIP        GQGTTLTVSS
```

Supplemental Figure 1. Alignment of the amino acid sequences from scFvs generated and tested in the study. The V-gene regions from the hybridoma for anti-DEC205 (NLDC-145) and anti-CD11c (N418) mAb were sequenced and combined with a linker into scFv. All the scFvs used in the study were aligned with ClustalW. Hyphen denotes gaps. The CDR loops are underlined based on analysis by IMGT/V-QUEST. The linker $(GGGGS)_3$ between the V_L and V_H is in bold.

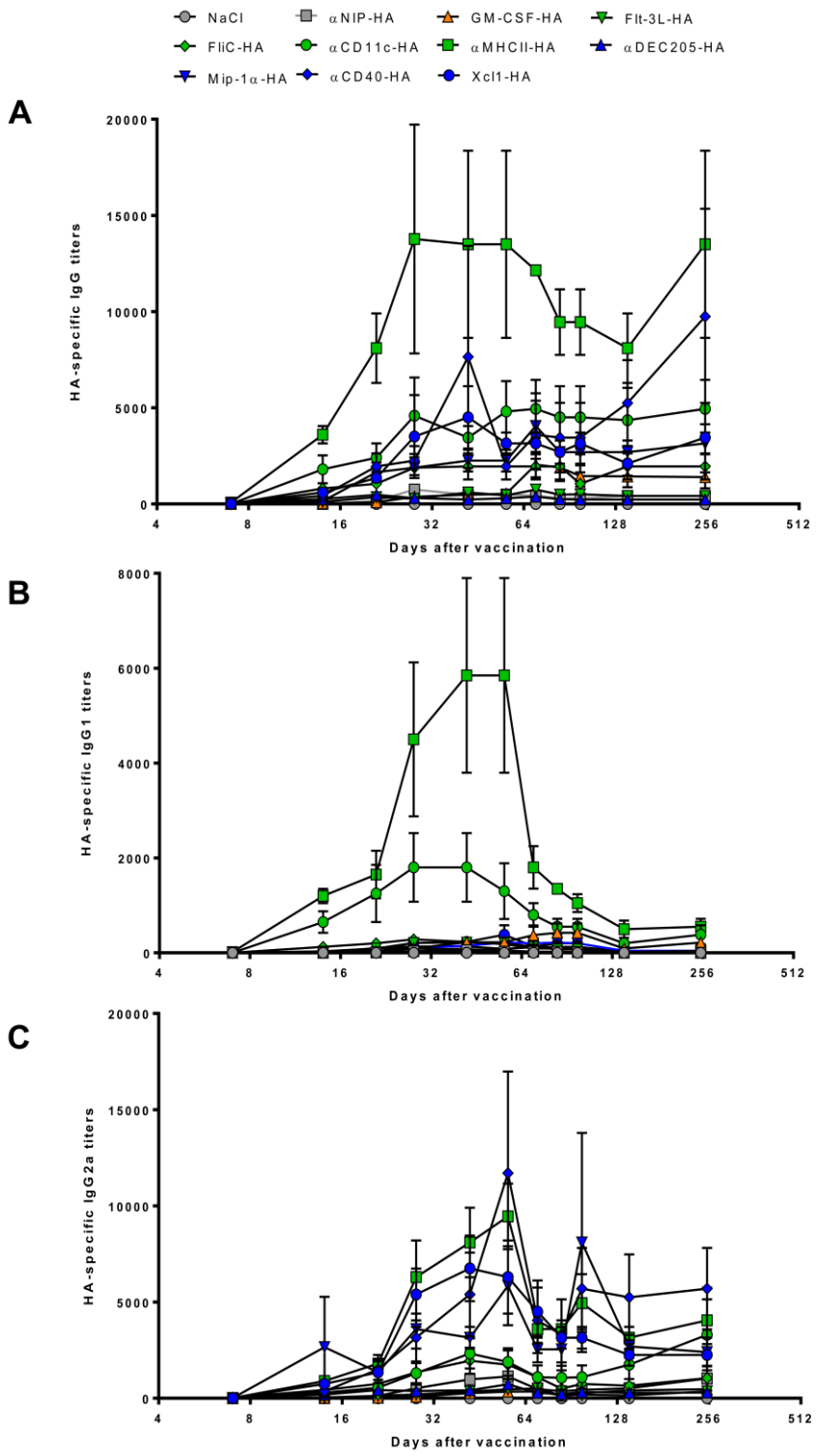

Supplemental Figure 2. A single DNA vaccination induced long-lasting antibody responses of IgG1 and/or IgG2a subclass. Each mouse was vaccinated with 25 µg DNA i.m. in each quadriceps followed by electroporation of the injection site. Serum obtained at various time points were analysed by ELISA. The ELISA shows HA-specific total IgG **(A)**, IgG1 **(B)** and IgG2a **(C)** for all the various targeted DNA vaccines (n=6, mean±SEM).

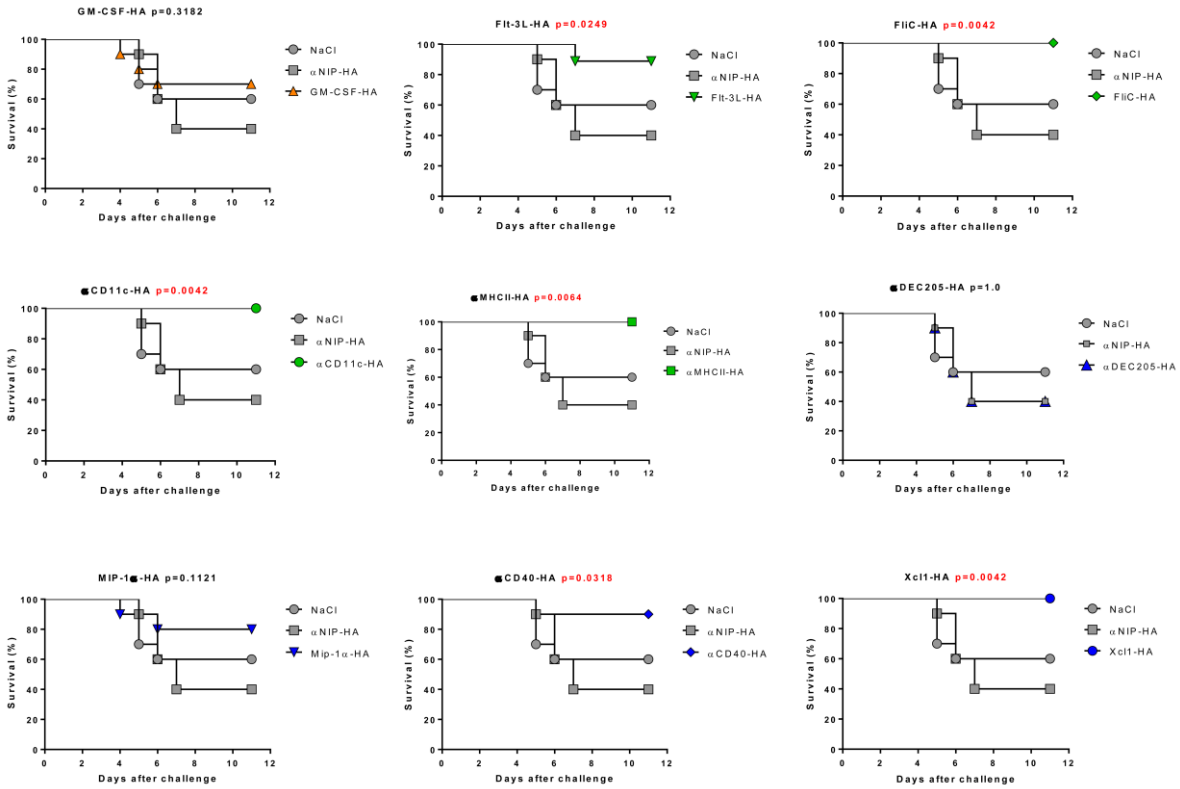

Supplemental Figure 3. Targeted DNA vaccination induced protection against nasal challenge with influenza virus after DNA vaccination. Mice were vaccinated with 25µg DNA i.m. in each quadriceps. After 14 days (n=10/group), mice were challenged with 5xLD^{50} of influenza A (PR8/H1N1) viruses and the weight monitored for 10 days. 20% weight loss was defined as humane endpoint at which time-point the mice were euthanized. Survival curves of the various targeted vaccines compared with NaCl and nontargeted vaccine αNIP-HA. Mantel-Cox analysis was used to compare targeted groups with nontargeted αNIP-HA. Significant p values are shown in red.

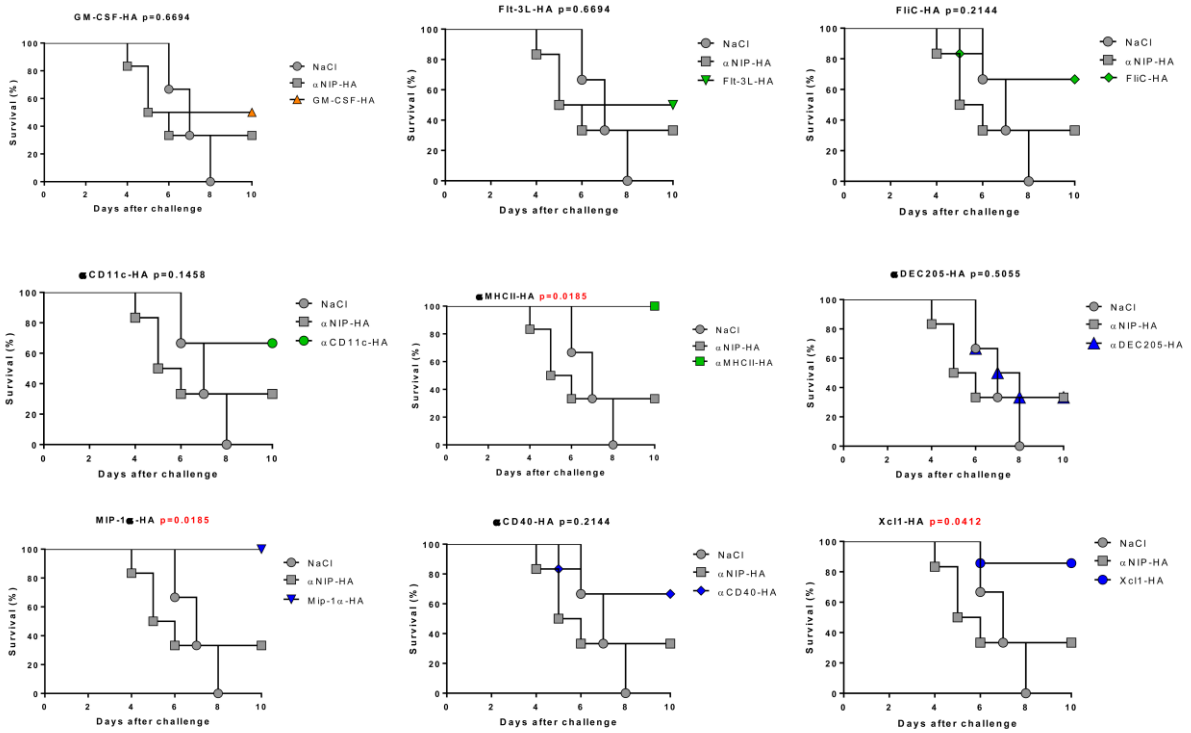

Supplemental Figure 4. Targeted DNA vaccination induced protection against nasal challenge with influenza virus after DNA vaccination. Mice were vaccinated with 25µg DNA i.m. in each quadriceps. After 252 days (n=6/group), mice were challenged with 5xLD^{50} of influenza A (PR8/H1N1) viruses and the weight monitored for 10 days. 20% weight loss was defined as humane endpoint at which time-point the mice were euthanized. Survival curves of the various targeted vaccines compared with NaCl and nontargeted vaccine αNIP-HA. Mantel-Cox analysis was used to compare targeted groups with nontargeted αNIP-HA. Significant p values are shown in red.